

# Journal Pre-proofs

Review

3D printing in biofabrication: From surface textures to biological engineering

Zeyu Ma, Jue Wang, Liguo Qin, Alex Chortos

PII: S1385-8947(24)07968-3

DOI: <https://doi.org/10.1016/j.cej.2024.156477>

Reference: CEJ 156477



To appear in: *Chemical Engineering Journal*

Please cite this article as: Z. Ma, J. Wang, L. Qin, A. Chortos, 3D printing in biofabrication: From surface textures to biological engineering, *Chemical Engineering Journal* (2024), doi: <https://doi.org/10.1016/j.cej.2024.156477>

This is a PDF file of an article that has undergone enhancements after acceptance, such as the addition of a cover page and metadata, and formatting for readability, but it is not yet the definitive version of record. This version will undergo additional copyediting, typesetting and review before it is published in its final form, but we are providing this version to give early visibility of the article. Please note that, during the production process, errors may be discovered which could affect the content, and all legal disclaimers that apply to the journal pertain.

© 2024 Elsevier B.V. All rights are reserved, including those for text and data mining, AI training, and similar technologies.

## 3D printing in biofabrication: from surface textures to biological engineering

Zeyu Ma<sup>1,2</sup>, Jue Wang<sup>2</sup>, Liguo Qin<sup>1\*</sup>, and Alex Chortos<sup>2\*</sup>

1. School of Mechanical Engineering, Key Laboratory of Education Ministry for Modern Design and Rotor-Bearing System, Institute of Design Science and Basic Components, Xi'an Jiaotong University, Xi'an, 710049, P. R. China

2. School of Mechanical Engineering, Purdue University, West Lafayette, IN, 47907, USA

Corresponding email: liguoqin@xjtu.edu.cn; achartos@purdue.edu

**Keywords:** 3D printing, texture, surface engineering, tissue engineering

### Abstract

On-demand printing through additive manufacturing (AM) has become a mainstream method for fabricating bio-inspired and biological systems. The rapid development of new printing approaches provides capabilities for prototyping precise 3D structures that recapitulate features of biological systems. To address challenges posed by the living environment, natural organisms have evolved a series of multi-purpose functional biomaterials and structures with properties such as super-hydrophobicity, anisotropy, and mechanical reinforcement. These provide rich inspiration for biological design and fabrication. Implantable organs with biomimetic surfaces and interfacial structures are created using 3D printing technology to further improve their compatibility with the human body and enhance their biomechanical properties. This paper reviews and summarizes the current structural designs and applications of bioprinting. We also explore a variety of different biomimetic surface-interface structure designs combined with 3D printing, highlighting and categorizing their applications. Finally, we discuss the optimized design of 3D printed biomimetic surfaces with functional materials, focusing on the opportunities and challenges in the field of bio-AM.

### 1. Introduction

Bio-additive manufacturing (AM) is an emerging technology in tissue engineering and regenerative medicine, facilitating the creation of tissue and organ-like structures. This method involves bioprinting models *in vitro*, which can then be transplanted into the body for predictive diagnostics and therapeutic applications.[1,2] Alternatively, bioprinting can be conducted directly *in situ* within the living body.[3] Both *in vitro* and *in situ* printing use 3D printing and its derivative technologies to create cell-containing objects with high resolution and layered tissues.[4,5] In overall biomanufacturing, not only is bioprinting included, but also the subsequent processes of proliferation and growth of cells in the tissue.[6] In addition to the

material properties of the printing ink,[7] the structure of the print building blocks can also significantly affect cell growth and proliferation.[8–10]

Different structures of the printed component implants have varying effects. To realize the printing of different structures, simply designing 3D models is not sufficient. This is because different printing methods focus on different priorities. The biggest advantage of the extrusion ink printing method is the adjustability of the ink (**Figure 1a, b**).[1,11] However, this method is far less precise than others, often resulting in complex models being printed with low precision.[12] Therefore, extrusion ink printing is commonly used in the field of biomanufacturing to print scaffold structures (which do not require high precision).[13] Scaffolds offer the advantage of providing a 3D framework that guides cell attachment and growth. Additionally, scaffolds can be designed with specific porosity, pore size, and connectivity.[2] These parameters can be adjusted to optimize the delivery of cells as well as the release of growth factors, which in turn maintains the activity and viability of the cells.[14,15] Furthermore, complex structures can be engineered to perform diverse functions and better adapt to the organism when implanted, necessitating the application of various 3D printing technologies (**Figure 1c, d**). Thin-walled, complex structures, including hourglass shapes and single columns with large aspect ratios, can be fabricated using laser-assisted printing.[16,17] Human corneal stroma featuring a dome structure,[18] along with intestinal scaffolds containing human chorion,[19] can be precisely printed using the stereolithography (SLA) method. Utilizing the high-precision capabilities of two-photon printing (TPP), multicellular microspheres featuring extremely small openings (at the micron level) on their surfaces were designed and printed to control the migration of cancer cells.[20] Corresponding to the needs of different implantation sites and tissues, specific 3D structures are necessary and can be selectively prepared using the appropriate printing technology.

However, these 3D structures often face challenges in ensuring optimal contact with the human body or other implant hosts, and their surface morphology may potentially disrupt the implant's functionality. For instance, when 3D printing a dental implant, the design includes microstructures that enhance its hydrophilicity, facilitating faster bonding with the body and accelerating wound healing.[21] Consequently, it is crucial to consider the fabrication of microstructures on implant surfaces to enhance properties such as superhydrophobicity,[22,23] superhydrophilicity,[24,25] self-cleaning,[26] antimicrobial activity,[27,28] wetting,[29] and friction resistance.[30,31] Certain organisms have developed complex structures featuring unique surface functionalities, encompassing specially evolved hierarchical structures ranging from the nanoscale to the macroscale.[32–36] These structures can be utilized as templates for interfacial surface designs in the development of next-generation bio-printed implants. For instance, lotus leaves, roses, and pine leaves exhibit exceptional superhydrophobicity and self-cleaning capabilities.[37–39] Additionally, the preparation of superhydrophobic surfaces inspired by the structures of springtails and geckos is facilitated through the use of TPP-based 3D printing (**Figure 1e**).[22] Cell adhesion properties can be customized by modifying the organ surface structure and selectively designing zones with hydrophobic and hydrophilic properties.[40,41] Simultaneously, the implementation of self-cleaning surfaces facilitates bacteriostatic and antifouling effects.[42] An active antifouling method that reduces cell adhesion is achieved through the preparation of self-cleaning cylindrical membranes.[43] Cell adhesion, encompassing attachment to substrates, spreading, and cytoskeleton development, on the modified surface can be effectively modulated by altering its wettability properties (**Figure 1f**).[44] Additionally, changing the surface's wettability also influences the amount of protein adsorption, which is advantageous for tissue engineering applications.[45] Furthermore, the ribbed structure of shark skin significantly reduces hydrodynamic drag, thereby dramatically enhancing its swimming speed.[26,46] Implants used in cardiac and vascular surgeries,

including artificial blood vessels and heart valves, which possess drag-reducing properties on their surfaces, can decrease turbulence and friction during blood flow.[47] This reduction in turbulence and friction subsequently lowers the risk of thrombosis and improves blood compatibility.[48] These findings confirm that by modulating the surface structure of implants to provide various functions, and subsequently applying them to the appropriate organs and tissues, they can significantly contribute to tissue engineering applications (**Figure 1g, h**).

Therefore, this perspective commences with an introduction to bioprinting technology, detailing the different methodologies currently available for bio-AM. It then assesses which specific aspects of tissue engineering are best addressed by each printing technique, aiming to provide the reader with a clear understanding of the advantages and disadvantages associated with each method. The design, processing, and fabrication of bionic surface textures are subsequently explored, with an emphasis on their integration with 3D printing technology. This comprehensive overview enables readers to more effectively choose the appropriate printing technology to enhance surface texture printing accuracy and shape fidelity. Lastly, the critical role of 3D-printed surface textures in biological tissue engineering is discussed, and the concept of ‘surface-tissue’ interaction is introduced as a novel paradigm for advancing next-generation bioprinting, particularly in enhancing the *in vivo* properties of implants through surface texturing.

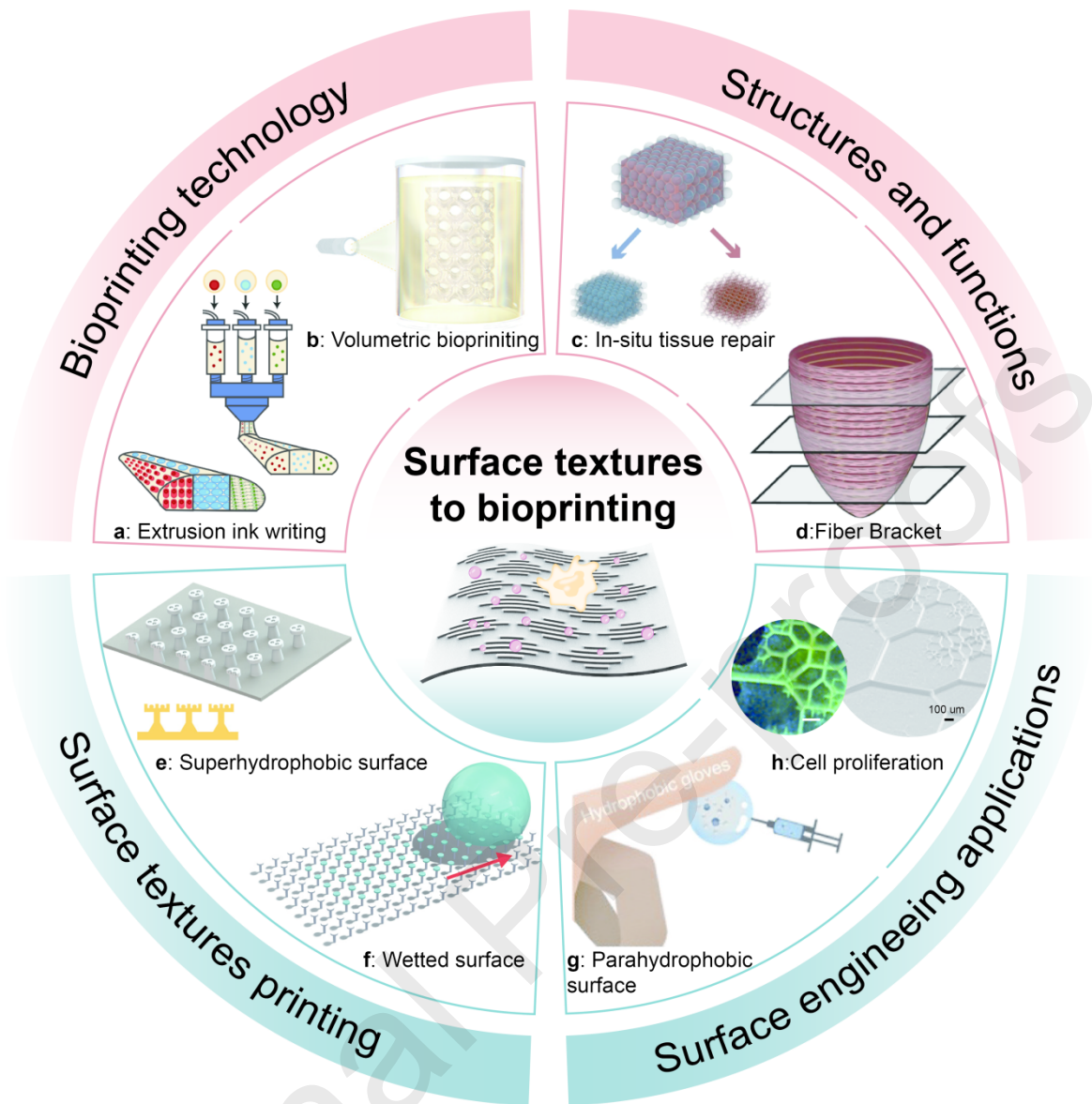


**Figure 1.** From surface textures to bioprinting. Different bioprinting techniques: a) direct ink printing;[1] b) volumetric bioprinting.[9] Functions performed by various printed structures: c) in situ printing of different structures;[3] d) gelatin fiber arrangement leads to different microstructures.[8] 3D printing for surface textures: e) TPP printing of superhydrophobic functional surfaces;[22] f) 3D printing wetting functional surfaces.[29] Applications of surface engineering: g) femtosecond direct writing for the preparation of parahydrophobic surfaces;[24] h) dynamic optical projection stereolithography to prepare surfaces favorable for cell proliferation.[49]

## 2. 3D bioprinting

3D bioprinting encompasses several core components: design, manufacturing, and application. The design process often incorporates bionics, while manufacturing typically involves self-assembly methods. Ultimately, the final printed products are biologically tested, either *in vivo* or *in vitro*. We discuss these in more detail below.

## 2.1. Biomimicry

Nature serves as an exceptional teacher, and through a lengthy evolutionary process, living organisms have developed a wide array of structures to continuously adapt to their environments. Biology-inspired engineering has effectively addressed numerous practical engineering challenges across various fields such as flight,[50,51] navigation,[46,52] materials science,[53] cell proliferation,[54] and micro- and nano-manufacturing.[55] Its application in bioprinting mainly consists of the fabrication of tissues or organs as well as their cells, involving the bionics of components as well as structures. For instance, bioprinting can replicate the functional components of specific tissue cells to achieve bionics, thereby mimicking the structure and function of real skin.[56,57] This is done by printing bioinks that contain multiple cell types, such as epidermal and dermal cells. Similarly, the function of heart muscle tissue can be bionically reconstructed by precisely controlling cell placement and tissue structure.[58] Moreover, artificial blood vessels, crucial tissue structures within the human body, can be fabricated using bioprinting technology to exhibit complex network structures. These vessels must structurally resemble natural blood vessels and functionally support blood circulation.[59] Additionally, the creation of porous bionic scaffolds, which facilitate bone repair and regeneration by working in concert with bone cells, mimics the natural growth environment of bone, promoting cell growth and bone formation.[2,15] More advanced applications of biomimetic bioprinting involve printing complete organs, such as kidneys or livers, for transplantation.[8] This technique faces the challenge of replicating the complex multi-cell type structures and functions of these organs. The various biomimetic designs discussed, from replicating biological tissues at the microscopic scale to designing biological organs at the macroscopic scale, necessitate a deep understanding of cellular behavior in microenvironments and the integration of suitable printing techniques to achieve them.

## 2.2. Different printing approaches and applications

The principal technologies employed in bioprinting include inkjet printing,[60] extrusion ink printing,[61] laser-assisted printing,[62] and stereolithography printing (**Figure 2**).[63] Additionally, several other printing technologies represent modifications and enhancements of these. Consequently, the selection of a bioprinting method is contingent upon specific requirements such as resolution, cellular activity, material properties, and structural characteristics.

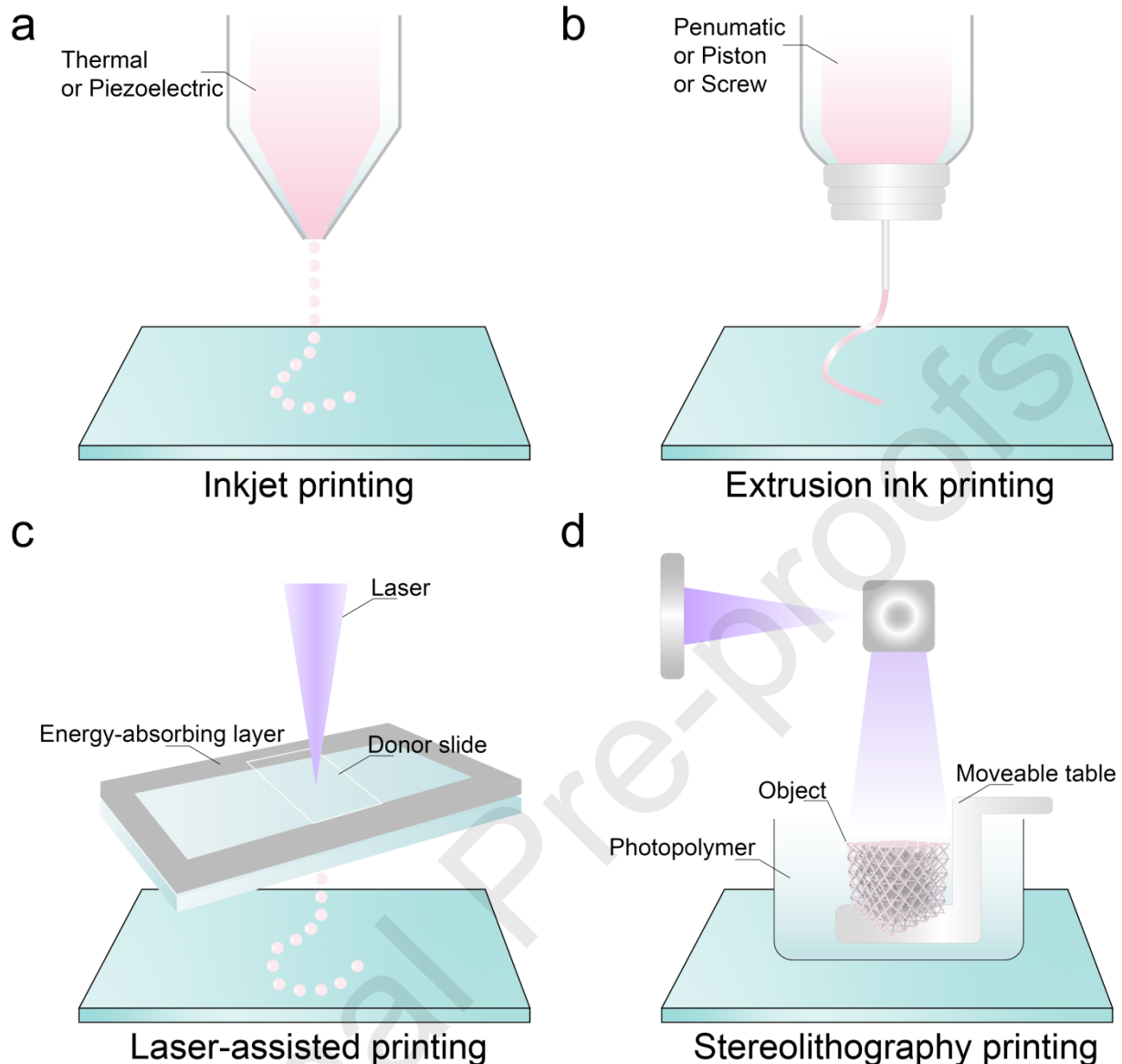


**Figure 2.** Components of inkjet, extrusion, laser-assisted bioprinters and stereolithography bioprinters. a) Inkjet printers with different stimulus (thermal or electrical) responses. b) Extrusion ink printers with different extrusion methods (pneumatic, piston, screw). c) Laser-assisted printers utilize a laser focused on an absorbing substrate to generate pressure to propel the cell-containing material onto a collector substrate. d) Stereolithography printers fabricate porous scaffolds by selectively illuminating photopolymers with a light source.

### 2.2.1. Inkjet printing

Inkjet bioprinters offer significant advantages such as low cost, high speed, and compatibility with a wide range of biomaterials.[64] For instance, these printers can create compositionally heterogeneous structures by varying the density and size of the ejected droplets, which allows for modulation of concentration gradients of cells, growth factors, and other components within the 3D structure.[65] Additionally, this technology supports more accurate biomimicry and regulation in designs that emulate actual living organisms. Compared to other more sophisticated bioprinting technologies, inkjet bioprinting devices are generally less expensive and simpler to disseminate and implement, enabling many

laboratories to modify and enhance these systems freely, building upon conventional 2D inkjet printing technology.[64] This technology is extensively employed by numerous teams to advance the capabilities of inkjet bioprinters. The enhancement of high resolution in inkjet printing primarily targets the precision of droplet size and deposition volume. At present, it is feasible to achieve droplet volumes ranging from a minimum of 1 pL to over 300 pL,[66,67] with deposition rates ranging from 1 to 10,000 drops per second (**Table 1**).[68] Currently, a single small cell-filled droplet can print a pattern with a width of approximately 20 μm.[69] Future developments in inkjet printing should focus not only on improving the construction of complex 3D structures but also on maintaining the existing convenience.

### *2.2.2. Extrusion ink printing*

Extrusion ink printing operates by extruding a filamentary paste through a nozzle that builds up layers sequentially (**Figure 2b**), unlike inkjet printing, which generates droplets. The nozzle moves in the xy-plane to create a 2D pattern, while the z-axis console shifts to facilitate the addition of subsequent layers. Currently, this printing method is highly compatible with a variety of materials, including soft matter,[26,70] hydrogels,[8,14] biocompatible ceramics,[2,13,71] and cell-laden fluids.[61,72] Among the prevalent extrusion techniques (pneumatic,[73] mechanical piston,[74] and screw spinning[75]), the pneumatic approach accommodates the broadest range of ink viscosities and is particularly effective with more viscous inks, albeit with some delay. The mechanical piston method facilitates direct ink distribution but demands a more robust mechanical structure due to the viscosity requirements of the ink. Screw rotary systems offer precise spatial control for extruding high-viscosity inks, though they involve more complex mechanics. By contrast, pneumatic extrusion handles high-viscosity inks with simpler mechanics, constrained only by the capacity of its pneumatic system. Moreover, multi-material, multi-nozzle extrusion becomes feasible on a high-throughput platform utilizing multi-material, multi-nozzle adaptive 3D printing.[76] This platform can independently control nozzle heights and seamlessly switch between inks, applying three different visco-elastic inks to complex substrates with varied topographies, including those with surface irregularities akin to skin abrasions or deep grooves. This capability opens new possibilities for the rapid patterning of soft materials in structural, functional, and biomedical applications. One of the advantages of extrusion ink printing is its ability to achieve higher cell densities compared to inkjet printing. Higher cell densities are particularly beneficial for specific tissue applications, such as heart and brain.[77,78] This technique has been employed to fabricate various tissue types, including aortic valves, branching vascular trees, in vitro pharmacokinetics models, and tumor models.

### *2.2.3. Laser-assisted printing*

Laser-assisted bioprinting devices need to have a complete pulsed laser light source as well as a focusing system (**Figure 2c**), using a laser to precisely control the release of bioinks. The laser beam is focused onto a small spot on the surface of the bioinks, generating enough energy to vaporize or create tiny bubbles in a small portion of the ink. This localized energy input causes an increase in pressure on the ink and pushes it out to the desired location. By controlling the position and intensity of the laser, the shape and position of the released bioink can be precisely controlled.

The precise control of the laser beam in LAB enables the printing of biomaterials with exceptional precision and resolution, facilitating the creation of complex structures and microscopic features. The resolution is primarily influenced by factors such as laser energy, the surface tension of the ink, substrate wettability, and the bioink's thickness and viscosity.[62,79] Furthermore, the LAB printing process is generally faster than traditional

bioprinting methods as it does not require direct contact with the biomaterial, thereby reducing printing times. The absence of nozzles eliminates clogging issues associated with ink viscosity mismatches. LAB is compatible with a wide range of viscosities, from 1 to 8000 mPa/s,[80,81] and its non-contact nature prevents physical damage to cells, thus preserving their integrity and functionality. Additionally, LAB technology enables precise control over cell location and distribution within biomaterials, enhancing cell survival and viability. LAB can deposit cell densities of  $10^8$  cells/ml with microscale resolution, achieving individual cell placement per drop at speeds up to 1,600 mm/s, and utilizing a laser pulse repetition rate of 5 kHz.[82] Moreover, LAB supports the use of diverse biomaterials, including cells, cell carriers, and scaffolds, enabling the fabrication of more complex and functional biological tissues and organs.[83,84]

#### *2.2.4. Light curing printing*

SLA boasts numerous advantages in bioprinting, particularly in creating biological structures such as tissue engineering scaffolds and microfluidic chips. This technology enables the printing of extremely fine and intricate structures, crucial for replicating delicate biological models. For instance, using SLA combined with computed tomography angiography data, 3D models of blood vessel structures with diameters of 400  $\mu\text{m}$  and resolutions as low as 25  $\mu\text{m}$  have been fabricated. These models are instrumental in studying the mechanisms of arterial thrombosis—a major cause of heart attacks and strokes—and developing therapeutic strategies.[63] Additionally, SLA supports a wide array of light-cured biocompatible materials, including hydrogels and specific bioactive substances,[85,86] producing structures with smooth surfaces that enhance cell attachment and proliferation. Conversely, DLP excels in rapidly curing entire layers of material, facilitating large-scale and rapid production.[87,88] DLP devices generally incur lower operating and equipment costs compared to SLA and are better suited for large-scale production due to their ability to process multiple structures simultaneously. For example, large-scale hydroxyapatite porous bioceramics (length >150 mm) with highly micro- and nano-porous surface structures (print resolution <65  $\mu\text{m}$ ) have been successfully fabricated using DLP. This demonstrates DLP's capability to produce large bone tissue engineering scaffolds with precise porosity.[87] Recent advancements in SLA include the development of near-infrared (NIR) 3D bioprinting, which enables non-invasive *in vivo* 3D bioprinting.[89]

**Table 1.** Comparison of different bio printing technologies

|                            | Bioprinting technologies type                               |  |                                  |   |
|----------------------------|---|--|----------------------------------|---|
|                            | Inkjet printing   | Extrusion ink printing   | Laser-assisted printing          | Light curing printing                         |
| Material Viscosities       | 1.7~300 mPa*s[90,91]  | 30 mPa/s to $6 \times 10^7$ mPa*s[77]                                  | 1~8000 mPa*s[80,81]              | SLA 100~1000 mPa*s<br>DLP 30~150 mPa/s[92,93] |
| Molding methods            | Chemical, photo-crosslinking[66]                            | Chemical, photo-crosslinking, shear thinning, temperature, solvent[94] | Chemical, photo-crosslinking[84] | Chemical, photo-crosslinking[95]              |
| Preparation time           | Low[96]   | Low to medium[96]  | Medium to high[97]               | High[86]                                      |
| Printing speed             | Fast (1~10,000 droplets per second, 10~1000 mm/s)[68]       | Slow (3100 mm/min)[98]   | Medium-fast (200~1600 mm/s)[82]  | Fast (4000 mm/s)[99]                          |
| Resolution or droplet size | <1 pl to >300 pl droplets,[66,67] 20 $\mu\text{m}$ wide[69] | 5 $\mu\text{m}$ to millimeters wide[100]                               | <1 $\mu\text{m}$ [101]           | 8~10 $\mu\text{m}$ [102]                      |
| Cell Viability             | >90%[103]   | 73.6%~92%[104]   | >95%[105]                        | >90%[106,107]                                 |

|                          |                            |                             |                                  |   |
|--------------------------|----------------------------|-----------------------------|----------------------------------|---|
| Cell densities           | Low, $10^6$ cells/ml[108]  | High, cell spheroids[109]   | Medium, $10^8$ cells/ml[82]      | Medium, $1\sim 3 \times 10^8$ cells/ml[110] |
| Printing cost            | Low[77]                    | Medium[77]                  | High[77]                         | Low[111]                                    |
| Type of print structures | Simple, cell/scaffold[112] | Medium, scaffold/tissue[72] | Medium-complex, tissue/organ[80] | Complex, organ[9]                           |

---

## 2.3. Materials, structures and applications

### 2.3.1. Bioinks

3D bioprinting requires meticulous attention to cell viability, unlike other forms of additive manufacturing—such as those involving metals, ceramics, and thermoplastic polymers—that do not need cell-friendly environments. Traditional methods can employ processes harmful to biological cells, including the use of organic solvents, high temperatures, and cross-linking agents. In contrast, 3D bioprinting starts with bioinks that must be compatible with bioprinting technologies and suitable for subsequent structural design and functional realization.

Bioinks, which refer to materials containing cells for bioprinting, currently face several challenges. Physical and chemical perturbations, such as pressure encountered during bioprinting, may affect cell behavior and survival.[113] During printing, the cell density needs to be high enough to ensure the formation of multicellular structures in subsequent stages, while the content and survival of cells vary between printing methods (**Table 1**). The addition of cells can alter the properties of the final molded biomaterial, potentially causing toxicity to the cells.[114] In different bioprinting techniques, the concentration of the ink currently exceeds 1,000,000 cells/ml (**Table 1**). This cell concentration represents no more than 5% of the total volume of the bioink, and therefore does not significantly impact the rheological properties required for extrusion ink printing. Instead, extrusion ink printing induces a fluid state with low viscosity due to an increase in shear rate, i.e., shear-thinning properties.<sup>[101]</sup> This shear can cause some cell damage, so special attention is needed when using extrusion ink methods. In inkjet printing, cells that cluster can interfere with droplet ejection.[115] As the cell content increases, it poses a greater challenge for inkjet printing, which is why current inkjet printing inks have low cell content. For LAB, SLA and DLP printing, thermal damage from the laser light source and UV light exposure is a concern for ink safety.[116] Generally, a criterion is sacrificed, such as reducing cell viability or content, to achieve high-precision printing.

Therefore, it is of utmost importance that the bioink meets the requirements for cells to thrive and possesses the biocompatibility needed for long-term transplantation, proper swelling characteristics, and short-term stability.[80] Short-term stability ensures that a robust three-dimensional structure is maintained during printing and that the pores and channels within the structure are well-organized, allowing cells to attach, grow, and proliferate effectively.[96] Next, we will discuss in detail the importance of structure for bioprinting and the key properties, such as functional applications and material biomimicry, that different structures can provide.

### 2.3.2. Structure and corresponding applications

Different bioprinting methods have diverse applications in the biomedical field due to their unique characteristics. This section will provide an overview of recent advances in various bioprinting techniques, highlighting their technical features for preparing simple and complex structures in the biofabrication of cells and tissues, as well as their applications.

The structures that can be printed with inkjet printing are relatively simple compared to other printing methods, characterized by the low viscosity requirements of the bioinks and relatively fast printing speeds (**Table 1**). Bead-jet, a variant of inkjet printing, introduces new features. Bead-jet printers, specifically designed for high-throughput intraoperative formulation and printing of matrix gel beads containing mesenchymal stem cells (MSCs),

hold the promise of repairing severe trauma.[112] High-density encapsulation of MSCs in Matrigel beads enhances MSC function and increases MSC proliferation, migration, and extracellular vesicle production compared to low-density beads or high-density bulk encapsulation of the same number of MSCs. Printing structures with heterogeneous organization includes two types of gelatin microbeads, yellow and green (**Figure 3a-i**). This approach can improve tissue microenvironment simulation by patterning multiple types of cellular and tissue elements within an engineered architecture. This heterogeneous structure is relatively simple in three dimensions. Complex three-dimensional structures were printed, such as freestanding microvessels with endothelial cells embedded in fibrin tubes, using a single piezoelectric nozzle.[117] Microvessels were generated by continuously printing alginate-based droplets containing endothelial cells into a bath of viscous cross-linking agent (**Figure 3a-ii**). By first printing in a circular pattern, the alginate capsules bind to form a helical structure as the printed scaffold sinks, a process reminiscent of layer-by-layer extrusion printing. Rapid cross-linking of the alginate provides temporary structural support to guide fibrinogen polymerization into hollow tubes. Tiny blood vessels printed by this method can remain viable for more than 14 days. Further challenges include the design and preparation of complex structures, such as bionic designs articular cartilage.[118] MEW was first used to produce arrays of polymer structures that orient the growth of spontaneously generated cell aggregates and provide tensile enhancement to the resulting tissues. Inkjet printing was then used to deposit a specific number of cells into the MEW structures, which self-assembled into organized arrays of spheres over several hours, ultimately generating a hybrid tissue with a composition similar to transparent cartilage (**Figure 3a-iii**). Structurally, the printed cartilage mimicked the typical organization of tissues observed in skeletally immature synovial joints, with potential applications in biological joint surface remodeling. The most interesting and promising application for inkjet printing is brain tissue printing. Creating realistic brain-like tissue has always been a significant challenge due to the delicate nature of brain tissue. Using 3D printers to eject cells, some researchers have prepared tissues that look and behave similarly to brain blocks.[94,119] By modifying the printing technique, it is possible to print and combine multiple cell subtypes to better mimic signaling in the human brain (**Figure 3a-iv**). This new technique may offer advantages over existing methods used by neuroscientists to create 3D brain tissue in the lab.

Extrusion ink printing offers many advantages. One obvious advantage is the ability to print anatomically shaped structures based on clinical imaging data. This is well demonstrated by the bioprinting of cell-containing bioinks with supporting biodegradable polymers to design structures that resemble bone, cartilage, and skeletal muscle. Classical layer-stacked scaffold structures are widely used in clinical medicine (**Figure 3b-i**). Bone implants with interconnected large porosity and good mechanical properties were prepared by extrusion-assisted 3D printing, combining Sr<sup>2+</sup> ion-modified MgP ceramics and PCL polymers.[13] This combination significantly improved the range of applications for the materials. MgPSr-PCL30 implants were able to promote bone formation in vitro without the addition of osteoinductive components, and in vivo experiments demonstrated their effectiveness in promoting bone defect repair. The MgPSr-PCL30 implant not only provides a new combination of 3D printing materials for bone tissue engineering but also offers a new solution for repairing large and complex bone defects. Extrusion ink printing not only mimics the complex geometry of organs but also addresses the challenge of cells self-organizing into functional tissues within 3D structures (**Figure 3b-ii**).[8] Precise 3D printing requires no support material, thanks to the customized rheology of the ink, which allows for a controlled sol-gel transition. The shear-induced alignment of fibers during the printing process endows the final scaffolds with microscopic anisotropy, mimicking the extracellular matrix of cardiac tissue. This feature is critical for guiding human cardiomyocytes to self-organize into

anisotropic muscle tissue in vitro. This advancement opens new avenues for creating 3D printed tissue models with higher fidelity to natural tissue, offering promising prospects for biomedical research and therapeutic applications. Very interesting tissue adhesives can be prepared by extrusion ink printing, enabling the fabrication of bioadhesive patches and devices with programmable architectures, which opens up new possibilities for application-specific designs (**Figure 3b-iii**). The adhesive is malleable and stretchable, achieving a solid bond with moist tissue within seconds and demonstrating good biocompatibility.[120] In an *in vivo* rat model of tracheal and colonic defects, the printed patch demonstrated leak-proof tissue sealing ability and maintained adhesion for up to four weeks. Additionally, the introduction of a hydrophobic matrix that repels blood enabled the printed patch to seal living blood tissues. For *in vitro* applications, viscoelastic inks can be rapidly patterned on arbitrary 3D surfaces using the Multi-Material Multi-Nozzle Adaptive 3D Printing platform (**Figure 3b-iv**). This platform demonstrates the ability to conformally pattern viscoelastic inks on complex substrates, including those with surface imperfections that mimic skin abrasion or deep indentations, by independently controlling the nozzle height and seamlessly switching between different inks.[76] This technology overcomes the limitations of previous 3D printing technologies, which were largely restricted to flat substrates and single materials, and opens up new possibilities for applications such as structural defect repair, wound repair, and tissue regeneration.

LAB technology enables the printing of engineered tissues with high cell density and microstructures. Guillotin. achieved the first cell printing at 5 kHz and micrometer resolution, solving the problem of balancing resolution and speed simultaneously.[82] The precise arrangement of multiple cell types in a designed pattern during the same printing process was realized, providing a technological basis for future complex tissue engineering constructs in which multiple cell types coexist. A method capable of printing at high cell concentrations was developed to ensure that the printed tissues have cell densities similar to those of natural tissues (**Figure 3c-i**). The advantages of laser-assisted bioprinting technology in terms of high resolution, high speed, and multi-cell type tissue printing were experimentally verified. However, the technology has not yet achieved structures identical to actual tissues and organs, remaining on the scale of tiny structures. In addition, corneal-like tissue structures can be constructed using LAB technology.[84] Using recombinant human laminin and human type I collagen as the basis of bioinks, three types of corneal structures were printed: stratified corneal epithelium, lamellar corneal stroma, and composite structures containing both stroma and epithelial portions (**Figure 3c-ii**). The construction of three-dimensional corneal structures was successfully realized. These bioinks are biocompatible with human stem cells and facilitate the construction of corneal tissues with potential clinical applications. The printed corneal structures exhibited good mechanical properties without additional cross-linking, demonstrating feasibility in porcine corneal organ culture and providing new ideas and techniques for future corneal regenerative medicine. Further, free-form 3D printing of alginate and cellular tubular structures, including complex Y-shaped tubes and cantilever structures, can be performed using LAB technology (**Figure 3c-iii**).[121] Under optimized printing conditions, the cell survival rate remained high immediately after printing and after 24 hours of incubation, demonstrating good protection of cells during the printing process. The use of a crosslinking solution as support material solved the support problem in cantilever structure printing and simplified the printing process. This advancement supports the realization of complex structure printing and provides new technical ideas for applications in tissue engineering and regenerative medicine. As the technology continues to iterate, *in situ* printing has become more sophisticated, allowing bone regeneration to be promoted *in vivo* by generating pre-vascularized networks with defined architectures through *in situ* printing of endothelial cells in mouse cranial defects. For the first time *in vivo*, Olivia et al. achieved pre-

vascularized networks with defined architectures using LAB technology, significantly promoting bone regeneration.[122] Under optimized printing conditions, the cells had a high survival rate after *in vivo* printing, demonstrating the advantages of LAB technology in terms of biocompatibility and cell protection (**Figure 3c-iv**). Compared with random seeding, *in situ*-printed human umbilical vein endothelial cells significantly improved vascularization and bone regeneration rates in the cranial defect region, especially under disc-shaped and cross-circular pattern conditions. This implies that the same printing method and materials with different printing structures can have completely different implications for biomedicine, realizing different properties. Therefore, in the field of bioprinted tissues and organs, both the macroscopic three-dimensional structure and the microscopic surface structure have a significant impact.

The DLP technique allows the preparation of large-scale hydroxyapatite porous bioceramics over 150 mm in length, featuring micro and nano-scale surface pore structures (**Figure 3d-i**).[87] The micro/nanopore structure of the ceramics can be precisely controlled by adjusting the solids content of the printing ink and the sintering temperature, thereby optimizing the bioactivity of the material. *In vitro* and *in vivo* experiments demonstrate that these bioceramics have good bone regeneration ability, showcasing their potential for application in bone tissue engineering. The ceramics possess both macroscopic and micro-nano pore structures, and this bilayer structure facilitates protein adsorption and cell attachment, promoting osteogenesis and providing a new strategy for bone tissue engineering and the development of personalized bone implants. SLA has significant advantages in printing scaffold structures, particularly for preparing scaffolds with dual driving forces to achieve efficient cellular uptake and high-density cellular loading, which are critical in spinal cord injury repair (**Figure 3d-ii**).[123] The preparation of scaffolds with microstructures combining macroscopic swelling forces and microscopic capillary forces significantly improves the efficiency of cellular uptake. The designed and printed structure facilitates long-term storage and transportation and can be quickly used in clinical emergencies, demonstrating its great potential as an efficient cell delivery tool. DLP also enables the printing of more complex 3D structures. For example, complex organ structures, including highly intricate brain and heart structures, have been constructed using silk fibroin-based bioink, demonstrating the wide range of applications for silk fibroin-based bioink and DLP technology in tissue engineering and regenerative medicine (**Figure 3d-iii**).[124] Biocompatible hydrogels with multiple vascular networks and functional vascular topologies can also be created using SLA.[125] Complex vascular networks, including helical structures, Hilbert curves, bicontinuous cubic lattices, and annular junctions, were designed using a mathematical space-filling topology algorithm and generated in hydrogels by projected stereolithography (**Figure 3d-iv**). Functional vascular structures in hydrogels, such as venous valves and fluid mixers, were also validated, demonstrating the functionality of these structures *in vitro* and *in vivo*. The potential of these hydrogel structures in treating liver injury was demonstrated through experiments in a mouse model, providing new ideas for future tissue engineering and regenerative medicine applications.

Different printing methods have unique characteristics for biological applications, but the primary goal is to achieve functional consistency with shape similarity. After printing an implant, the first consideration is its interaction with the body upon implantation. Good contact not only ensures the stability of the implant but also minimizes its impact on the patient. How can the surface contact of the implant be improved? This can be achieved through bionic design of the implant surface, taking inspiration from natural plant and animal surfaces to prepare different microstructures that realize various functional surfaces. This approach will enhance the stability and biomechanical properties of the implant in the body.

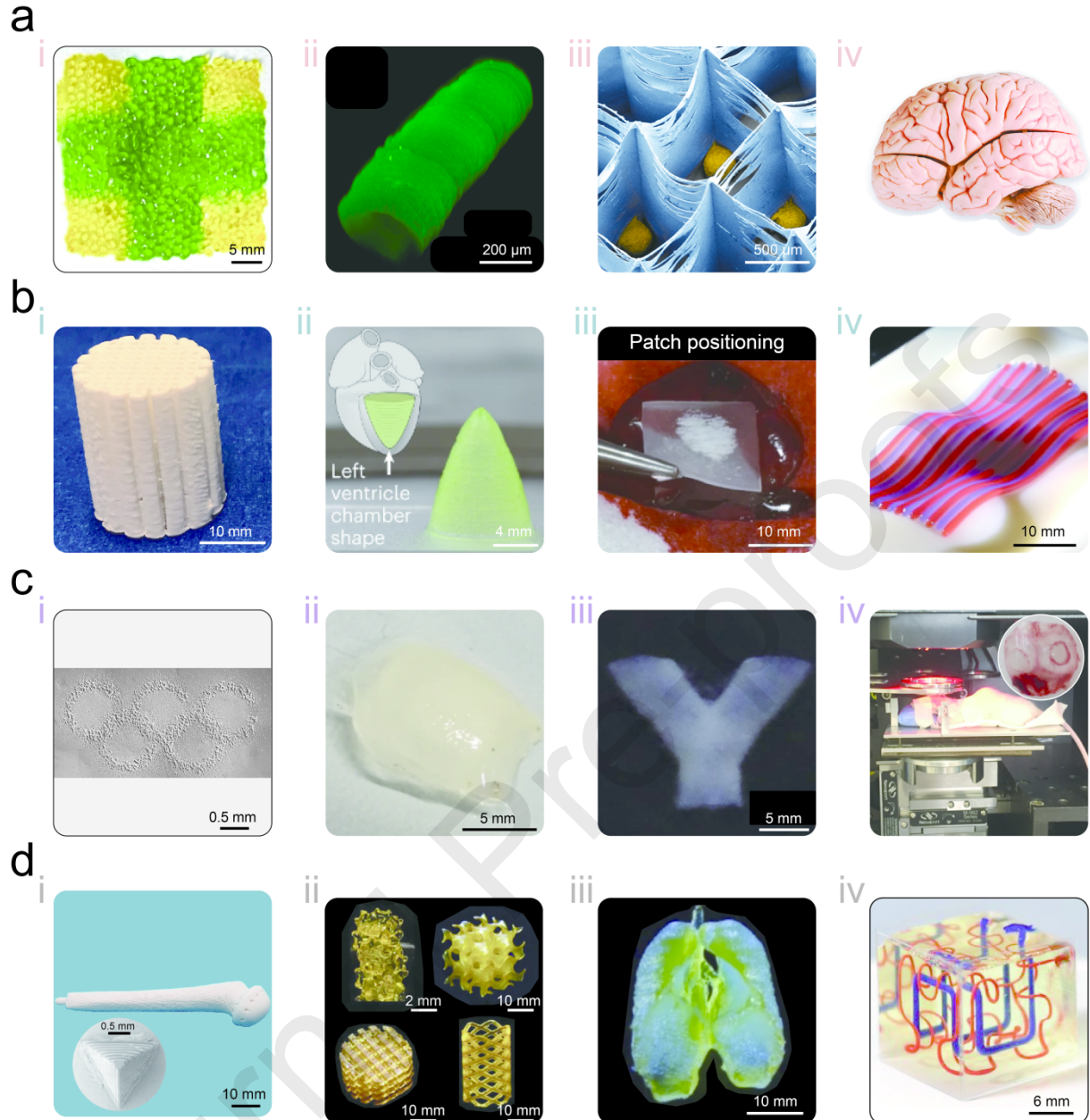


**Figure 3.** Bioprinting structures and corresponding applications. a) Inkjet printing for various structures, ranging from simple to complex.[112,117–119] b) Extrusion ink printing for complex structural applications, including biological scaffolds and fractal surfaces.[8,13,76,120] c) LAB, ranging from 2D cell deposition to direct generation of complex structures *in situ*.[82,84,121,122] d) SLA and DLP printing, covering applications from large bone structures to micronized vascular models.[87,123–125]

### 3. Surface textures printing

#### 3.1. Bio-inspired design and manufacturing

Different organisms in nature have evolved diverse surface structures to adapt to their environments. For example, the lotus leaf exhibits a superhydrophobic effect due to multilevel microstructures called “papillae” on its surface, which increase the surface contact angle and

prevent contamination by mud (**Figure 4a, c**).[26] The nepenthes vase features an annular lip around its entrance, covered with tiny grooves that guide prey toward the vase opening, increasing the likelihood of them slipping off the edge; this can be utilized as a liquid guide (**Figure 4b, d**).[126] The fine bristle structure mimicking the gecko's foot enables free crawling on smooth vertical surfaces.[127] A ribbed structure modeled after shark skin can reduce fluid resistance, enhancing speed and efficiency underwater.[46] Layered nanocomposite structures inspired by shells provide high stiffness and toughness, making them suitable for bulletproof materials, robust building materials, and wear-resistant coatings.[128] These examples illustrate the design of bionic multi-scale surfaces. Bionic interfacial structures represent a multidisciplinary research field involving physics, chemistry, materials science, biology, and other disciplines. This field's outstanding feature is the close integration of basic and applied research, reflecting the diversity of bionic concepts and material preparation techniques.

In recent years, researchers have conducted in-depth studies on several key scientific issues related to the construction and application of bionic multi-scale micro-nano-structures, achieving significant advancements and developing various surface structures to realize different functions (**Figure 4e, f**).[24,129] Among these advancements, bionically prepared superhydrophobic interfaces have evolved into multifunctional applications, including the simultaneous combination of different types of specific wettability, such as superhydrophobic/superoleophobic (superbiphobic), superoleophilic/superhydrophilic (superbiphilic), and superhydrophobic/superoleophilic.[130] By analyzing and theorizing the characteristic structures of different organisms, similar structures are designed and fabricated to achieve these specialized functions. This approach represents the overall logic of current biomimetic interfaces. Drawing on the unique structural surfaces found in nature, artificially oriented mimicry to prepare similar biological surfaces has become a breakthrough direction in the scientific community. Unique surface bionic structures have emerged and are rapidly being realized and applied to varying degrees. In today's era, biomimetic surface materials have become indispensable in various high-tech fields such as modern defense and military, industrial applications, environmental protection, and daily necessities.[131,132] For example, micro-nano manipulation of liquids and applications in the field of biomedicine can be realized through liquid delivery systems (**Figure 4g, h**). Currently, the study of surface structural properties is a prominent area of focus in materials science research.

The utilization of 3D printing technology for surface texturing preparation dates back to 2008.[133] Initially, "mushroom field" surface textures were printed onto ceramic abrasives and subsequently transferred to metal castings. The application of 3D-printed surface textures to orthopedic implants was later proposed to enhance osseointegration by increasing surface porosity and pore size, offering a valuable alternative to traditional biological fixation methods. Since then, the use of additive manufacturing techniques to prepare surface-interface textures with special functionalities has advanced significantly. Superhydrophobic surfaces with volumetric structures have been prepared using DLP printing technology, where nano-voids formed by porogenic solvents confer superhydrophobicity to the printed objects (**Error! Reference source not found.a-i**).[134] These objects exhibit extremely low water adhesion and retain their superhydrophobic properties even after wear and tear. The feasibility of printing superhydrophobic 3D objects has been verified, offering new ideas and technical support for integrating interface functionalities into entire objects. Drawing on the complex microstructure of the leaves of the aquatic plant *Salvinia molesta*, a superhydrophobic structure with eggbeater-shaped microhairs was designed and printed using FDM, exhibiting excellent superhydrophobic properties (**Figure 4e**).[135] An efficient oil-water separation method was developed to rapidly absorb and separate various oils, demonstrating its potential

application in environmental protection and the petroleum industry. Additionally, by adjusting the number of arms and spacing of the eggbeater structure, the droplet adhesion force can be controllably adjusted, showing significant advantages in droplet manipulation and microreactor applications. The potential of bionic superhydrophobic structures for droplet manipulation and oil-water separation has been experimentally verified, providing new material and technical support for environmental engineering and biomedical fields.

In recent years, 3D printing technology has made significant strides in the fabrication of functional surface structures, opening new avenues for the development of bionic materials and smart surfaces.[136,137] Traditional surface preparation methods, such as photolithography and etching, face limitations in creating complex geometries and multifunctional surfaces. In contrast, 3D printing enables the fabrication of intricate micro- and nanoscale structures by building materials layer by layer. This increased design flexibility not only allows for the more accurate mimicry of complex natural surface structures, such as shark skin, lotus leaves, and butterfly wing scales, but also facilitates the creation of surfaces tailored to specific application needs.[37,136] Current research on 3D-printed functional surface structures primarily focuses on several key areas. The first is material diversity and functionalization. The range of 3D printing materials has expanded beyond thermoplastics to include photosensitive resins, metals, ceramics, and multi-material composites.[26,137–139] This expansion allows researchers to fabricate functional surfaces with diverse physical, chemical, and biological properties, such as superhydrophobicity, antimicrobial activity, conductivity, photonic crystals, and surfaces with adjustable friction coefficients.

With advances in 3D printing, particularly in micro/nano-scale techniques like TPP and nanoimprinting, researchers can now fabricate higher-resolution surface structures. These techniques enable the production of complex structures at the submicron or even nanoscale, leading to more biomimetic and functionalized surfaces.[140–142] Additionally, 3D printing has advanced smart surface research by incorporating responsive materials (e.g., shape memory alloys, thermotropic materials, and photoresponsive materials) into the printing process, enabling the creation of dynamically tunable surfaces that respond to external stimuli, such as temperature, light, or humidity.[143,144] These smart surfaces hold promise in applications such as sensing, actuation, and self-cleaning.

The preparation of functional surfaces using 3D printing technology has become a significant branch in the field of bionic surface science, with numerous related studies. For example, TPP-printed bionic adhesion microstructures have been designed to combine springtail and gecko-inspired microstructures, exhibiting superhydrophobicity on both top and side surfaces and strong dry adhesion.[22] Another combination involves octopus suction cups and gecko-inspired microstructures, which exhibit excellent adhesion properties in both dry and wet environments. Additionally, a cactus- and nepenthes-inspired fog collector was designed and fabricated using customized micro-continuous liquid interface printing technology.[145] The fog collector consists of cactus-shaped spines with longitudinal ridges and a bottom channel with curved-inclined-arc pits and grooves (C-IAPGs). The C-IAPGs structure utilizes a combination of gravity, Laplace pressure gradient, and capillary forces to achieve fast and efficient water transfer, significantly enhancing droplet transport speed and efficiency. Furthermore, a surface mimicking the barb-like structure of the spiny flatfish (Filefish) skin was fabricated using DLP technology.[146] This surface, consisting of hook-like spines and rigid or flexible support layers, realizes frictional anisotropic properties similar to those of biological prototypes, making it suitable for applications such as smart sensors and specific tribological uses. These examples confirm the significant potential of 3D printing for surface interfaces. Next, we will present an overview of the different functional applications of current bionic surfaces to explore more ideas applicable in the field of bioengineering.

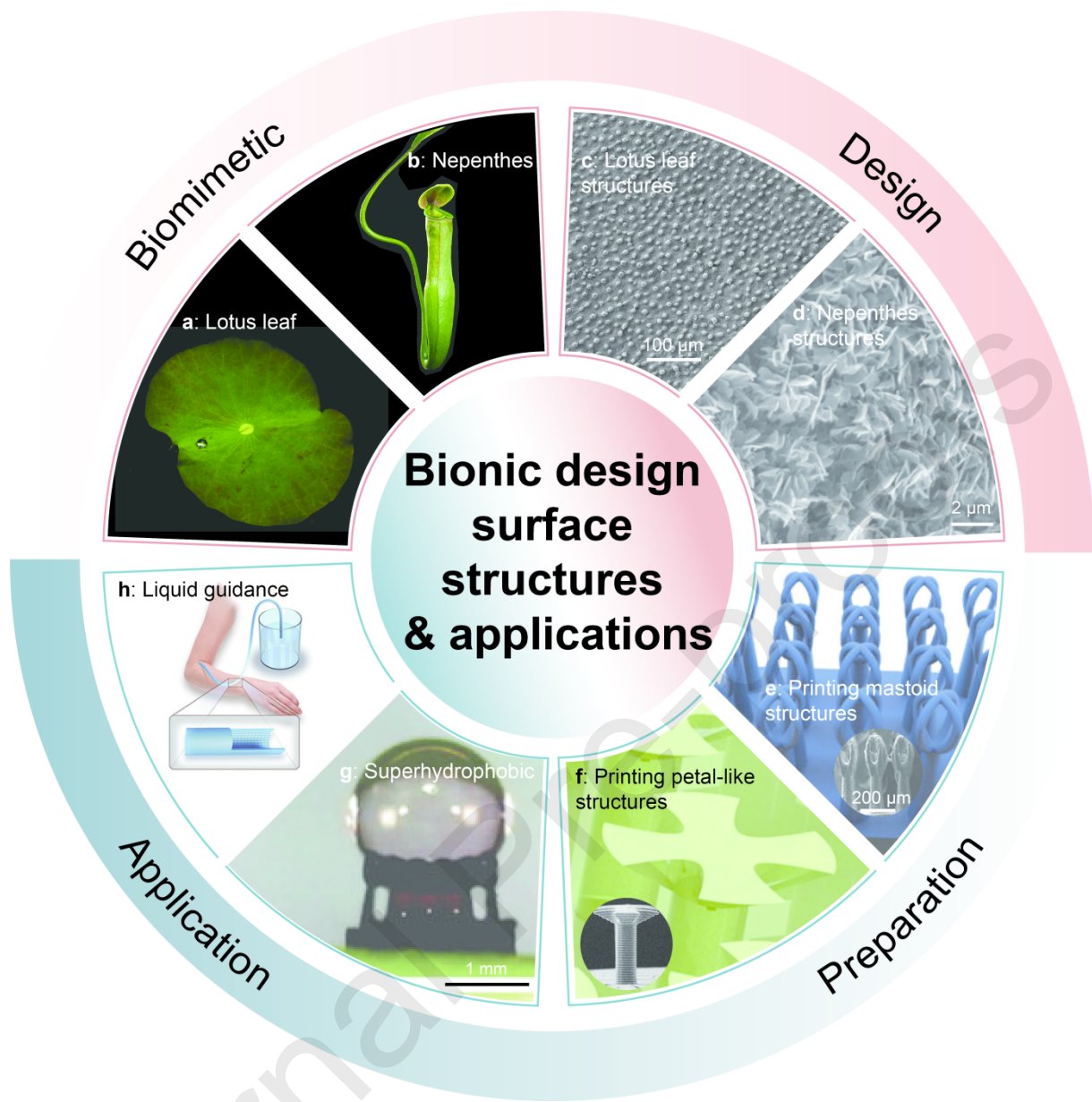


**Figure 4.** Bionic design surface structures and applications. a, b) Biological blueprints, such as those derived from lotus leaves and nepenthes, are utilized in bionics.[26,126] c, d) Microstructure of bionic blueprints.[26,129] e, f) 3D printed bionic structures.[135,147] g, h) Different applications of 3d printed bionic structures. [135,148]

### 3.2. Applications of textures

Bionic surfaces can be expanded into various directions and fields of application due to the different physical micro- and nanostructures that impart diverse functions. Examples include superhydrophobic surfaces (**Figure 5**), superhydrophilic surfaces (**Figure 6**), liquid-guiding surfaces (**Figure 7**), multi-functional surfaces (**Figure 8**), self-cleaning surfaces (**Figure 9**), adhesive surfaces (**Figure 10**), antimicrobial surfaces (**Figure 11**). Many of these surfaces interact with liquids, and since the main component of the human body is water, the adhesion, growth, and reproduction of cells are closely related to water. Implants in the human body can incorporate different functional surfaces to achieve better performance.

### 3.2.1. Superhydrophobic surface

With advancements in nanotechnology, new methods for fabricating superhydrophobic surfaces, such as laser processing, templating, and electrochemical deposition, are continually emerging.[149] These techniques have significantly improved the controllability, stability, and functionality of superhydrophobic surfaces. A key focus of current research is the long-term durability of these surfaces, which remains a challenge due to the demanding conditions in practical applications, including mechanical abrasion and chemical corrosion. Conventional superhydrophobic materials often struggle to retain their performance over extended periods in such environments. Consequently, researchers are developing more robust superhydrophobic materials by incorporating multilayer structures and nanocomposites to enhance durability.[26,150] While superhydrophobic surface interfaces are now very well developed, researchers such as Levkin et al. have advanced this technology to three-dimensional structures by utilizing DLP to print complex shapes (**Figure 5a**).[134] Through ink photopolymerization phase separation, a bicontinuous 3D structure with nanopores is formed, imparting superhydrophobic properties. It was also found that the nanopores were uniformly distributed and retained their superhydrophobic properties after wear tests. This advancement provides a foundation for the development of superhydrophobicity from surface interfaces to the three-dimensional scale. Chun et al. utilized a commercial FDM 3D printer and polylactic acid (PLA) filament to print surface structures with microscopic patterns.[151] The printed samples were then dip-coated with a mixed solution containing hydrophobic silica nanoparticles and methyl ethyl ketone to form a hydrophobic coating with nanostructures. These dip-coated 3D printed samples retained their superhydrophobic properties after five months of storage, demonstrating good long-term stability (**Figure 5b**). However, compared to the previous DLP one-piece molding method, this secondary dip-coating process is significantly more complex. Similarly, Ravi et al. prepared PLA superhydrophobic surfaces using FDM 3D printing combined with a chemical etching process.[151] This method, which does not involve nanoparticles, simplifies the fabrication process and avoids the complexity and environmental issues associated with nanoparticles (**Figure 5c**). It forms superhydrophobic surfaces with hierarchical structures and is simpler, more efficient, and economical compared to the secondary dip-coating of nanoparticles. Superhydrophobic products with complex configurations can be accurately constructed into functional bionic yarns with diameters of 900 µm using Two-photon Femtosecond Laser Direct Writing (TFLW).[24] The bionic yarn consists of hollow round tubes, regularly arranged micron-sized papillae, and nano-folds on the papillae surfaces, inspired by rose petals (**Figure 5d**). Compared to other natural and artificial hydrophobic materials, the bionic yarn exhibits excellent properties, including a higher contact angle and stronger droplet adhesion, demonstrating the great application potential of 3D-printed bionic yarn in functional textiles. Additionally, this technological approach can be used to develop products for bioengineering applications, such as superhydrophobic band-aids, which protect wounds from water and accelerate the recovery process.

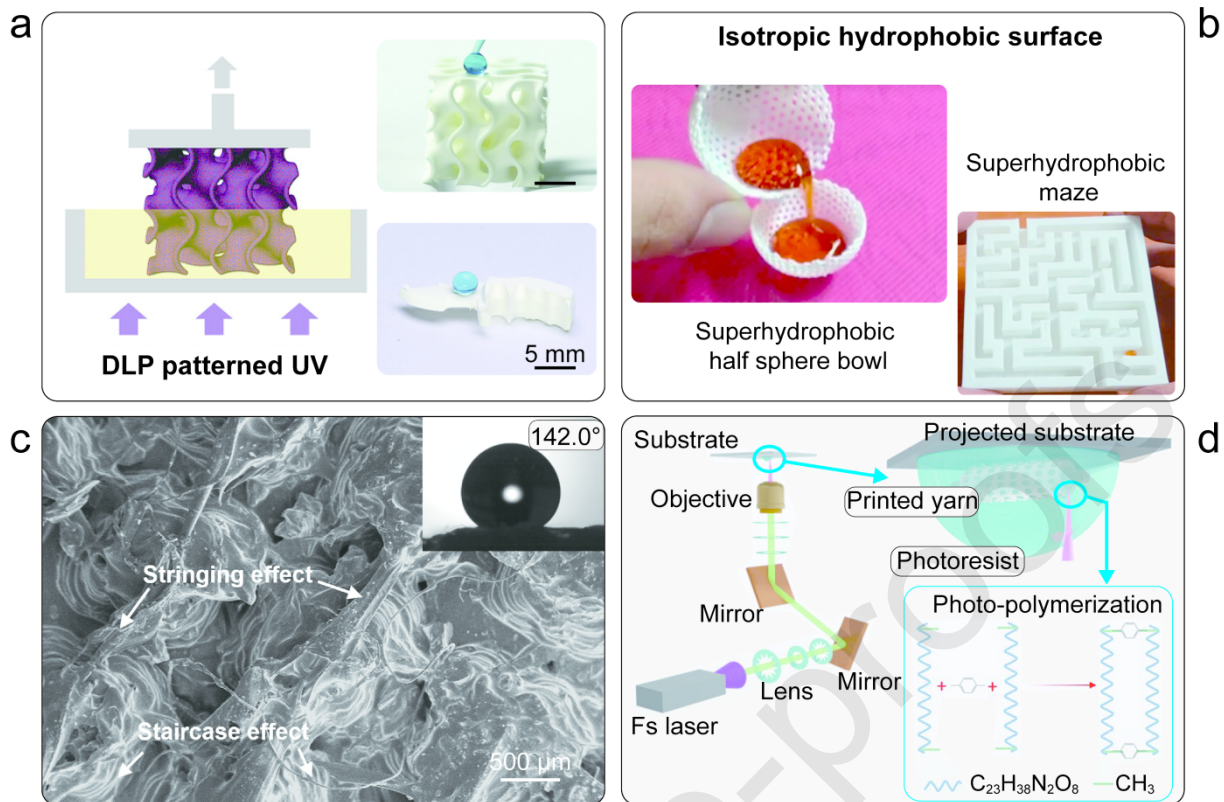


**Figure 5.** Applications of superhydrophobic surfaces. a) Superhydrophobic objects with bulk nanostructure.[134] b) Fabrication of a superhydrophobic surface using a FDM printer.[23] c) 3D printing and chemical etching a PLA surface.[151] d) Schematic of 3D printed parahydrophobic functional textile with a hierarchical nano-microscale structure.[24]

### 3.2.2. Superhydrophilic surface

Superhydrophilic surfaces are also a significant branch of biomimetic surfaces. Superhydrophilic surfaces demonstrate pronounced hydrophilicity by rapidly adsorbing water and forming a uniform water film. The primary characteristic of a superhydrophilic surface is its ability to quickly disperse and absorb water droplets, preventing them from aggregating or flowing.[40,152] This property offers potential advantages in various practical applications. One physical preparation method involves microstructuring, which enhances hydrophilicity by increasing surface energy through roughness modulation (e.g., a combination of nanostructures and microstructures). Common techniques include laser treatment, plasma treatment, and micro/nanofabrication. Zhao et al. fabricated superhydrophilic multifunctional Janus foams using spatially shaped femtosecond laser processing, which enables efficient fog collection and water transport.[130] This technology provides new material and technical support for addressing water shortages and pollutant detection (**Figure 6a**). Additionally, this hydrophilic surface treatment can be applied to human bioengineering, where hydrophilic treatment on the surface of new implants enhances cell adhesion and proliferation. Huang et al. prepared micro- and nanocomposite porous structures using in situ laser deposition, where the microstructures promote liquid wetting and the nanostructures inhibit organic diffusion.[152] The duration of superhydrophilicity was increased by a factor of 54 compared to conventional nanostructured surfaces (**Figure 6b**). Through molecular dynamics simulations and experimental studies, the structural design was optimized to ensure effective liquid wetting and organic diffusion inhibition, even when the outer layer is contaminated with organic matter. Revealing the mechanism of superhydrophilicity persistence and proposing novel preparation techniques provide new ideas and methods for the design and

fabrication of high-performance wetting structures. Superhydrophilic surfaces are more suitable for application in organisms than superhydrophobic surfaces, as the hydrophilic properties are more favorable for cell growth. Su et al. prepared superhydrophobic materials with anisotropic water transport ability and wear resistance through selective laser sintering (SLS) printing (**Figure 6c**).[153] Glass beads and thermoplastic phenolic resin powder were combined to construct superhydrophobic structures in a single step using SLS. During the printing process, long capillary channels formed, enabling anisotropic water transport on different print surfaces. These materials rapidly absorb water in a direction perpendicular to the print surface, while water absorption occurs more slowly on the print surface itself. This unique property allows the materials to resist gravitational water transport effectively. Abrasion tests demonstrated that the superhydrophobicity remained stable even after prolonged wear, showcasing excellent mechanical durability. The ability for directional liquid transport makes these materials promising for applications in the human body, such as nutrient delivery. Li et al. investigated a 3D-printed solar evaporator based on natural molecules.[154] Through rational structural design, they constructed a durable interfacial solar evaporator using inexpensive and efficient natural polyphenols, such as ellagic acid, combined with iron, thereby avoiding the environmental issues commonly associated with the synthesis of conventional photovoltaic materials (**Figure 6d**). The surface of the evaporator features a tapered array structure that significantly enhances light capture via multiple reflective and anti-reflective effects. This design also promotes efficient droplet collection and shows promise for application in external medical devices. Research on superhydrophilic surfaces is currently in a phase of rapid development, with future innovations and breakthroughs anticipated in material design, preparation methods, and functionalization. These advancements will also provide a stronger foundation for 3D printing superhydrophilic surfaces in bioengineering.

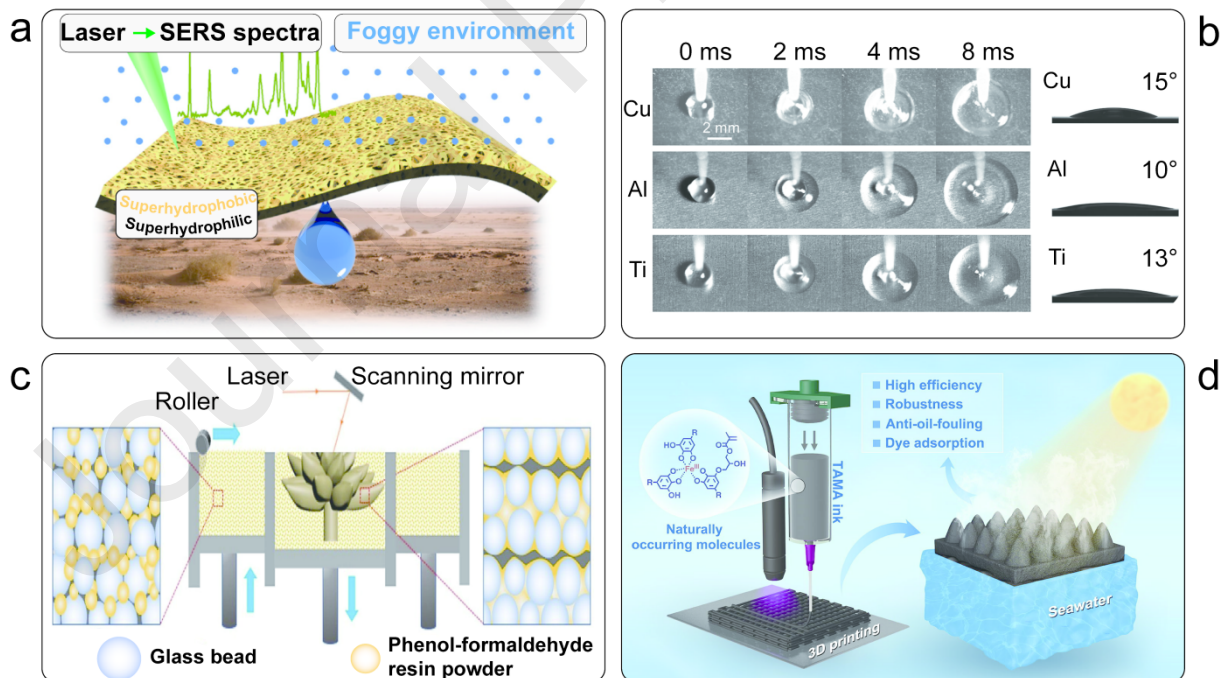


**Figure 6.** Applications of superhydrophilic surfaces. a) Superhydrophilic janus foam fabrication using a spatially shaped femtosecond laser.[130] b) Schematic of fabrication durable superwetting/superhydrophilic metal surfaces.[152] c) Superhydrophobic materials with anisotropic water transport capacity and wear resistance.[153] d) 3D-printed conical array solar liquid collector.[154]

### 3.2.3. Liquid-guiding surfaces

In addition, biomimetic surfaces play a significant role in liquid guidance and fractal structures. By mimicking biological surfaces in nature with efficient liquid management capabilities, such as those found in lotus leaves, desert beetles, and fish scales, researchers have developed artificial surfaces with unique liquid-guidance properties that significantly enhance the precise manipulation of liquids on surfaces.[155] Li et al. investigated a programmable 3D-printed bionic wheat awn structure system designed for efficient droplet collection.[156] Inspired by the wheat awn, the researchers developed a hierarchical bionic system incorporating tapered spines, gradient microgrooves, and oriented spines (**Figure 7a**). These combined structures enabled the system to excel in droplet capture and rapid transport. The bionic design facilitated a seamless transition from droplet capture to fast transport, significantly enhancing collection efficiency. The study also suggests that the bionic system can be applied to various shapes and assembly forms, offering innovative possibilities for the future development of multifunctional and efficient droplet collection devices. These devices are expected to be applied in bioengineering, such as in nutrient delivery for regenerating transplanted organs. Greer et al. drew inspiration from cactus thorns to design tree-like microstructures, using 3D printing to fabricate polyvinyl alcohol/polypyrrole hydrogel membranes with these tree-like structures.[157] The membranes efficiently capture fog droplets and evaporate them under sunlight (**Figure 7b**). This research introduces new ideas for developing more efficient liquid collection devices with promising applications. Other natural biological structures, such as spider webs, can also be mimicked through 3D printing to improve liquid collection efficiency. Furthermore, the introduction of 4D printing technology, which utilizes smart materials to create dynamic water collection devices that respond to environmental changes, expands the functionality and application potential of traditional water collection systems. Stellacci et al. constructed a super-wetting nanowire membrane using a self-assembly method, which can preferentially adsorb oil substances in water with an adsorption capacity of up to 20 times its own weight, exhibiting remarkable selectivity and high-efficiency adsorption performance.[158] The nanowire membrane can be resuspended in solution and recover its original paper-like morphology after multiple cycles (**Figure 7c**). It can be regenerated through ultrasonic cleaning and high-temperature treatment after several uses, showing good mechanical stability and heat resistance (up to 380°C). This innovative material demonstrates great potential for oil removal and can be effectively applied to wounds contaminated with oil in trauma surgery for controlled wound cleaning. Song et al. developed a new superhydrophilic tandem pendulum pattern (SSCP) inspired by the microcavity shape of a porcupine.[159] The water transport velocity of SSCP was found to be faster than that of the superhydrophilic tandem wedge pattern under the same parameters, and the faster water transport mechanism was analyzed (**Figure 7d**). Experimental results show that the water transport velocity of SSCP can reach 289 mm/s. This speed was achieved through a combination of one-factor experiments, orthogonal optimization design, streamline connection transition optimization, and pre-wetted patterning strategies. The optimized SSCP demonstrates excellent performance in long-distance water transport, gravity-resistant water transport, heat transfer, and fog collection, providing a new approach to high-performance fluid transport systems. Therefore, it can be used for fluid guidance in the human body.

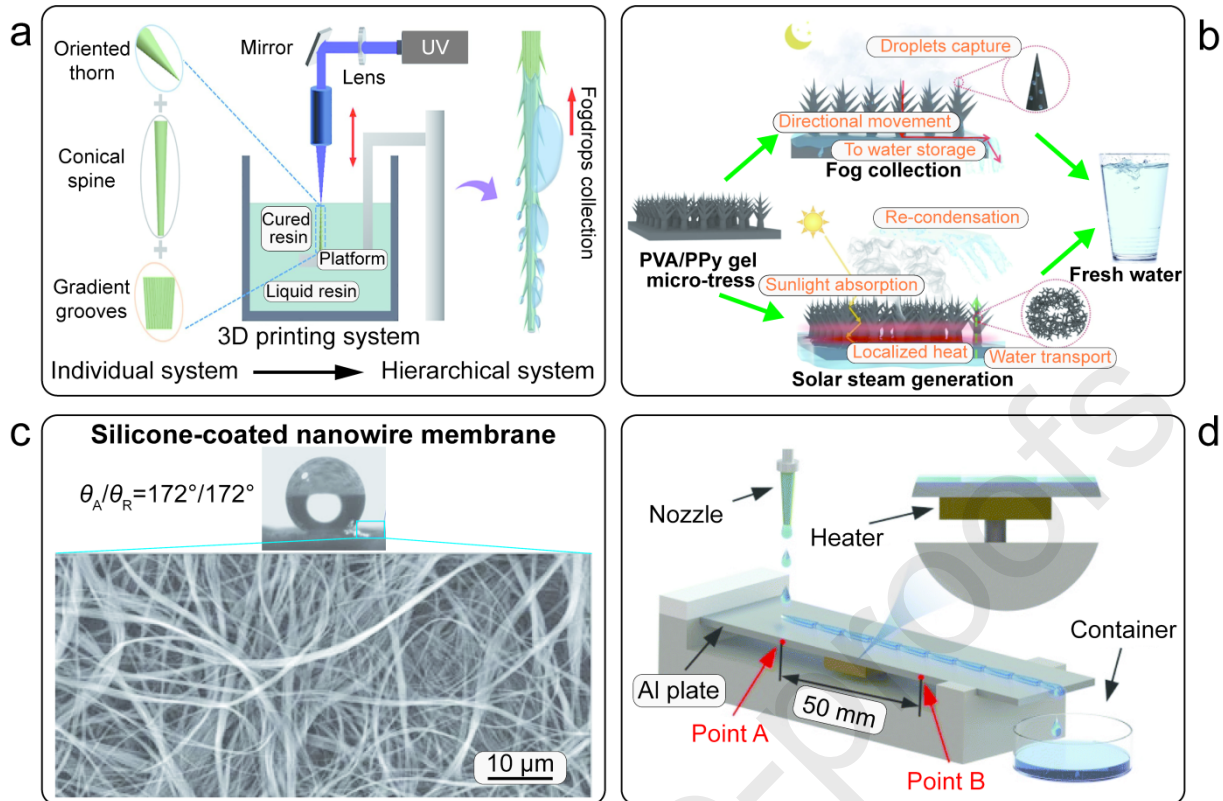


**Figure 7.** Applications of liquid-guiding surfaces. a) 3D-printed liquid collection system imitating wheat awn structures.[156] b) 3D-printed liquid-collecting membrane with a treelike structure.[157] c) Superwetting surfaces.[158] d): Enhanced water transportation on a superhydrophilic serial cycloid-shaped pattern.[159]

### 3.2.4. Multi-functional surface

Fractal structures, along with drag-reducing surfaces, represent an important branch of bionic surface design. Fractal structures are geometric formations characterized by self-similar properties across different scales. These structures are widely found in nature, such as in tree branches, blood vessels, corals, snowflakes, and lightning. A key feature of fractal structures is their ability to function at both micro and macro scales, providing a unique advantage in bionic surface design. The self-similar nature of fractal structures allows them to exhibit similar geometric features across multiple scales. This property enhances drag reduction by effectively dispersing and directing fluid flow, thereby minimizing resistance. The integration of fractal structures with drag-reducing surfaces is an effective biomimetic strategy for significantly reducing frictional resistance between fluids and solid surfaces. The drag-reducing effect of fractal structures is evident in many living organisms, such as sharks and dolphins, whose skin features certain fractal characteristics that contribute to reducing water flow resistance. Chen et al. successfully printed hydrogel scaffolds with complex fractal geometries for the first time using maskless stereolithography, transitioning from simple mathematical models to complex bionic fractal designs (Figure 8a).[49] By employing a DMD-based projection printing platform, they achieved micro-meter resolution and rapid fabrication, significantly improving printing efficiency and structural complexity. The biocompatibility and cell adhesion support of polyethylene glycol diacrylate hydrogels were demonstrated, with cell growth and proliferation on fractal structures further enhanced by fibronectin modification. These fractal geometries, resembling nature's patterns in optimizing energy and material distribution, show broad potential for tissue engineering and other biomedical applications. Liang et al. fabricated 3D-printed structures that mimic the surface

of shark skin and explored their drag reduction performance.[136] The unique surface texture of shark skin has long attracted the interest of biologists and engineers, and similar surface structures have been applied in various engineering and medical products. This study presents a method for evaluating the topographical parameters of shark skin and investigates the effect of scale orientation on hydrofluidic behavior (**Figure 8b**). Sharks-like surface structures with varying scale orientations were 3D-printed using acrylonitrile-butadiene-styrene materials. For the first time, the impact of scale orientation on the fluid damping performance of sharks-like surfaces was systematically examined, with results showing that the optimal damping effect occurred when the fluid flow direction was perpendicular to the scales. This study not only enhances the understanding of drag reduction mechanisms in sharks-like surfaces but also provides theoretical and practical insights for developing more efficient drag reduction technologies in the future. Furthermore, biomaterials used in long-term implants, such as artificial joints and cardiac stents, could be designed with sharks-like structures to reduce friction with body fluids or blood, minimizing discomfort and inflammatory reactions in patients.



**Figure 8.** Applications of multi-functional surfaces. a) 3D printing of hydrogel scaffolds with fractal geometries.[49] b) 3D-printed sharkskin-imitating surface structure.[136]

### 3.2.5. Self-cleaning surface

The development of superhydrophobic surfaces has gradually led to the creation of self-cleaning surfaces, which use their superhydrophobic properties to allow water droplets to easily remove surface debris as they roll. The microstructure of gecko skin demonstrates ultra-low adhesion of contaminant particles while providing a superhydrophobic, moisture-resistant barrier that can self-clean through low-speed rolling or impacting water droplets (**Figure 9a**). Watson et al. prepared a similar surface structure and material through bionic design, where small water droplets (10-100  $\mu\text{m}$ ) can easily enter the valleys between scales to achieve efficient self-cleaning.[127] These droplets can self-propel away from the surface, enhancing their mobility and cleaning effect. This study provides a new theoretical basis and technical support for the development of efficient self-cleaning surfaces, antimicrobial coatings, and biocompatible materials. Meanwhile, the contradiction between mechanical stability and hydrophobicity of self-cleaning surfaces can be resolved through dual-scale structural design. Deng et al. proposed a method to achieve superhydrophobic surfaces by constructing structures at two different length scales.[160] The microstructure provides mechanical stability, while the nanostructure provides hydrophobicity. The microstructure forms an interconnected surface framework containing “pockets” that hold highly hydrophobic but mechanically fragile nanostructures (**Figure 9b**). This framework acts as “armor” to prevent the removal of the nanostructures by abrasive materials larger than the framework size. The sidewalls of the microstructures are angled to enhance mechanical

stability while maintaining superhydrophobicity. This interconnected framework structure effectively protects the hydrophobic nanostructures from abrasive wear and maintains good self-cleaning performance, significantly improving the mechanical robustness of the surface.

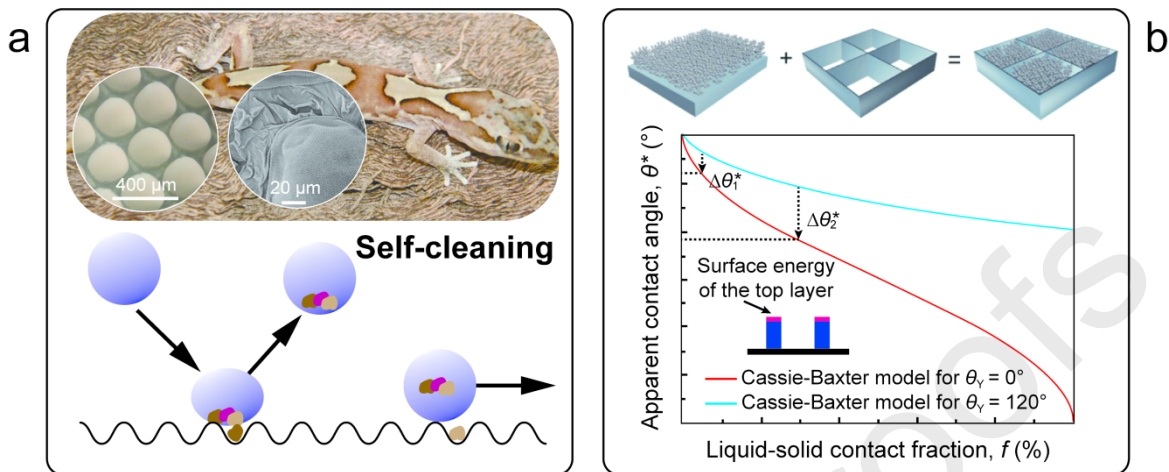


**Figure 9.** Applications of self-cleaning surfaces. a) Design of self-cleaning surfaces.[127] b) Schematic of self-cleaning structures.[160]

### 3.2.6. Antimicrobial surface

Research on antimicrobial surfaces has garnered significant attention in recent years, particularly in the medical, food processing, public health, and industrial sectors. These surfaces can effectively inhibit or kill microorganisms, such as bacteria and fungi, that adhere to the material's surface, thereby reducing the risk of infection and contamination. Gecko skin surfaces are antimicrobial against Gram-negative bacteria (*Porphyromonas gingivalis*), killing the bacteria on contact while showing good compatibility with human stem cells.[127] Antibacterial surfaces can also be prepared by mimicking gecko skin structures. Additionally, antimicrobial surfaces can be created using ZnO nano-arrays (ZnO NAs) structures. Zhou et al. grew ZnO NAs on stainless steel substrates using a two-step hydrothermal method.[161] The ZnO NAs exhibited ultra-fast physicobactericidal activity against *Escherichia coli* (E. coli) and *Staphylococcus aureus* (S. aureus), killing 97.5% of E. coli and 94.9% of S. aureus in less than one minute. The bactericidal mechanism was attributed to the high stress generated by the nano-array tips and irregular morphology, as supported by simulation analysis (**Figure 10a**). The renewable and photocatalytic self-cleaning function of the ZnO NAs surface was verified through cyclic sterilization experiments, maintaining high efficiency over multiple sterilization cycles. The ZnO NAs surface not only demonstrates excellent sterilization performance under laboratory conditions but also has a wide range of practical application potentials, including clinical therapy, water purification, and air filtration. High aspect ratio surface structures, present on the wings of organisms such as cicadas and dragonflies, exhibit significant antimicrobial effects (**Figure 10b**). These natural surfaces display unique antimicrobial activity by destroying pathogen cells through physical contact, independent of biochemical surface functions.[162] Such structures can be continuously optimized to enhance their biocompatibility and antimicrobial efficiency in applications such as biomedical implants. The optimized structures are printed in tandem with the implants using additive manufacturing, providing a safer and more effective material option for medical devices and other applications.

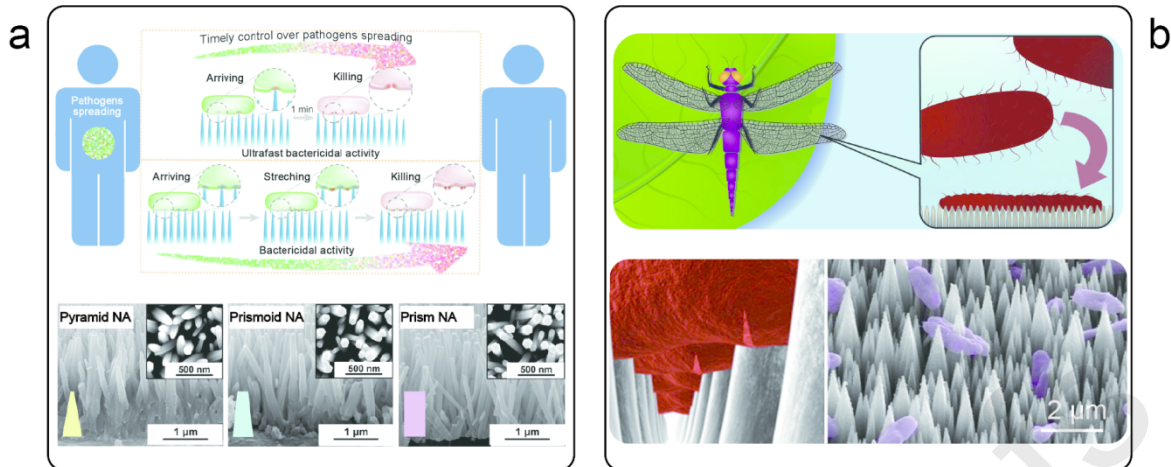


**Figure 10.** Applications of antimicrobial surfaces. a) ZnO nanoarrays for rapid and sustainable bactericidal applications.[161] b) Nano-structured antimicrobial surfaces.[162]

### 3.2.7. Adhesive and anti-wear surface

The choice of material for printing implants is critical, as friction properties directly affect biocompatibility. Low friction materials reduce wear and tear between the implant and surrounding tissue, thereby minimizing inflammatory reactions and adverse biological responses. Additionally, the stability of the implant in the body is closely related to friction. Appropriate friction can help the implant remain fixed in the target position during the initial phase without excessive movement or slippage. Conversely, high friction may lead to wear and tear of the implant material, shortening its service life. Bioengineering must consider the tribological properties of materials when designing implants to ensure their long-term functionality and durability. Chen et al. designed a strong wet friction surface enhanced by micro-nano hierarchies inspired by tree frog toe pads, aiming to achieve excellent wet friction properties without the need for special external forces.[163] This surface has potential applications in biomedical engineering, wearable flexible electronic devices, and other fields. The structural features of tree frog toe pads were replicated using micromachining techniques with polydimethylsiloxane (PDMS) materials. These structures exhibit strong boundary friction, with wet friction approximately 20 times greater than dry friction, without the need for special external forces. It was found that on the surface of the bionic structures, the liquid automatically splits and distributes uniformly to form a nanoscale liquid film, which generates strong boundary friction (**Figure 11a**). The self-splitting and self-absorption effects of liquids on the surface of micro- and nanostructures were discovered and verified, providing a new mechanism of liquid regulation. This understanding helps to optimize wet friction surfaces and offers theoretical support for the future design of bionic surfaces. Abalone shells exemplify excellent friction properties in nature, with a smooth interior suitable for contact with soft bodies and an outer layer providing strong mechanical properties that effectively protect the organism. Qin et al. utilized magnetic  $\text{Fe}_3\text{O}_4@\text{SiO}_2$  nano chains (NCs) reinforced composites, arranging the NCs differently in the surface layer of sensors to reduce the coefficient of friction and improve wear resistance through a combination of vertical magnetic field and extruded flow field (**Figure 11b**).[128] They investigated the effect of different NC arrangements on the mechanical behavior of polymers and found that vertically aligned NCs significantly increased the Young's modulus and hardness of the composites, while multilayer NC samples demonstrated the lowest hysteretic energy and the best mechanical properties. Low friction and high wear resistance were achieved through nano- and micrometer-scale structural design, particularly by using  $\text{Fe}_3\text{O}_4@\text{SiO}_2$  NCs alignment control to enhance material properties. Wang et al. designed bionic suction cups inspired by natural suction cup

structures, utilizing multi-material 3D printing technology to fabricate a bionic suction cup system with multi-level stiffness.[164] The system enables the rotation and movement of bionic scales through a soft body driver, achieving strong underwater adhesion. Its adhesion performance was verified on various surfaces, including smooth, rough, and flexible surfaces, demonstrating the bionic suction cup's ability to attach efficiently in complex environments (**Figure 11c**). This system holds significant application potential, particularly in the attachment of bioengineered transplanted tissues. Shao et al. designed flexible electrodes inspired by the red-netted tree frog, featuring high permeability, stable adhesion, and strong durability.[165] These electrodes aim to address issues of stable adhesion, low impedance, and durability in long-term continuous monitoring of physiological electrical signals. The electrode structure, modeled after the red-netted tree frog's toe pad, includes dispersed columns at the bottom and asymmetric tapered holes at the top (**Figure 11d**). This design improves contact stability through dispersed columns, showing a 2.79-fold improvement in adhesion under dry conditions and a 13.16-fold improvement under wet conditions. It also enhances breathability through an improved breathable channel structure, achieving a 12-fold improvement compared to cotton. The bionic electrode demonstrates good adhesion, low impedance, and strong durability under various skin conditions, making it suitable for long-term continuous detection of physiological electrical signals such as electrocardiograms, electromyograms, and electroencephalograms. In addition to excelling in medical health monitoring, the bionic electrode has potential for use as a 3D-printed implant with high adhesion.

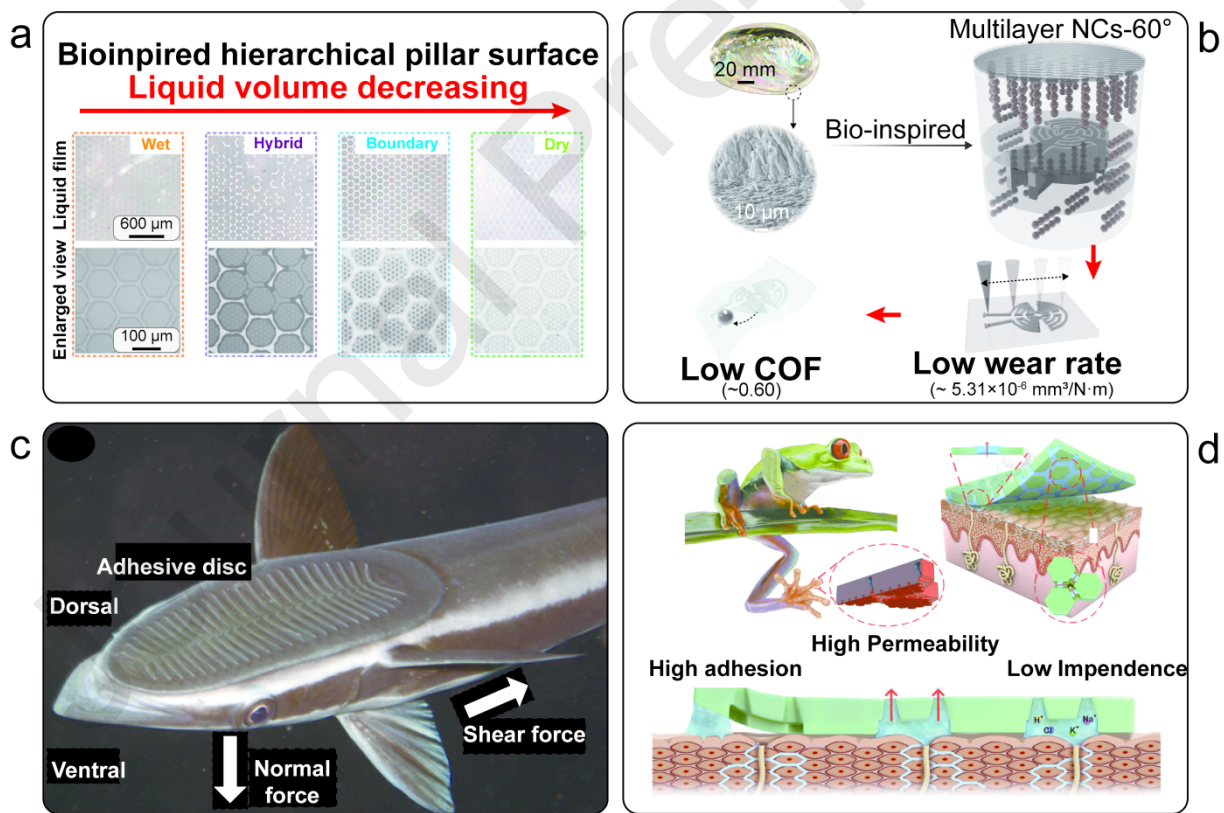


**Figure 11.** Applications of adhesive and anti-wear surfaces. a) Strong wet friction surface inspired by tree frogs.[163] b) Tree fog inspired surface with robust durability.[165] c) 3D-printed bionic suction cups.[164] d) Magnetically assisted 3D printed anti-wear surface inspired from abalone shell.[128]

#### 4. Surface textures printing into biological engineering

In the medical field, the utilization of biological surface structures has a long history. In drug delivery, for example, interfacial structures are designed to ensure secure attachment and prevent premature dislodgement of microneedles, thus ensuring precise delivery of the drug or therapeutic agent. Unlike traditional subcutaneous drug delivery, microneedling allows for painless administration.[132] However, smaller microneedles are prone to fracture. To address this, microneedles inspired by shark teeth, mosquitoes, and praying mantis forearms achieve higher adhesion, while those designed with reference to the barb of a honeybee's olecranon needle are more difficult to pull out.[166–169] These biomimetic surface designs enhance the reliability of drug delivery. Moreover, the science of surface biomimetics should not be limited to medical devices. Combining the structural properties of biological surfaces with additive manufacturing can offer advanced strategies for tissue engineering. In implant printing, the choice of print material and surface treatment significantly influences friction properties. Using 3D printing technology, the surface structure of an implant can be customized to optimize its frictional properties for specific bioengineering needs. For example, the surface friction properties of *in vivo* implants are regulated through the design of surface microstructures. By controlling the friction, the performance of the implant can be improved, such as by reducing resistance during implantation or increasing stability after implantation. The frictional properties of the implant also affect postoperative recovery. Appropriate friction promotes tissue healing and integration, while excessive friction may lead to tissue damage and postoperative complications.

##### 4.1. Surface textures in human organs

The skin, as the outermost structure of the human body, serves multiple roles as the first line of defense for human health, including physical, chemical, and immune barriers. In the event of burns or other skin damage, medical repair is required. Some biological surfaces in nature possess properties that can be applied to human skin (**Figure 12a**). For example, sharks, known for their excellent swimming abilities, have ribbed structures on their shield scales that alter water flow, reducing turbulence and fluid resistance.[46,52] This microstructure can also effectively remove surface dirt and microorganisms as water passes through, providing a self-cleaning effect. Such structures can be introduced to repair injured skin. Additionally, the surface of the tree frog features natural antimicrobial peptides and high adhesion properties,[163,165] which can be replicated through 3D printing to create bionic skin or wound dressings. These biomimetic solutions can reduce the risk of infection and promote wound healing, especially for burns and chronic wounds. Thorns typically have a sharp and hard structure to prevent damage or attacks by herbivores or predators.[131] Their surfaces are often rough and uneven, which not only enhances their defensive capabilities but also helps reduce water evaporation and resist microbial attacks. By using 3D printing to create thorn-like structures for bionic skin and soft tissue surfaces, their protective properties can be enhanced. This approach can be particularly beneficial in trauma repair and surgery, improving tissue recovery and protection. The abalone has a tough outer shell that can withstand great external forces, with the cross-arrangement of the pearl and prismatic layers providing excellent mechanical properties.[170,171] Altering the orientation and distribution of reinforcing particles in composites can enhance their mechanical properties in the direction of mechanical loading. Inspired by this, composites can be designed to adapt the distribution of materials in three dimensions, mimicking the structure of abalone shells. This local customization results in anti-wear materials, serving as a blueprint for fabricating biomimetic skins for long-lasting artificial skin applications. Our previous work has confirmed that structural materials modeled after abalone shells exhibit excellent tribological properties.[128]

The papillary structure on the surface of the lotus leaf provides excellent self-cleaning properties.[37] This multi-stage structure creates extreme hydrophobicity, allowing water droplets to carry away dirt and bacteria as they roll over the surface, keeping it clean. When applied to medical devices such as urinary catheters, this structure can reduce the risk of scaling and bacterial infections, improving patient comfort and safety (**Figure 12b**). It also facilitates catheter insertion and removal, reducing tissue damage and enhancing patient comfort. The antibacterial properties can be further enhanced by adding antibacterial materials or coatings to the lotus leaf papillae structure, effectively preventing bacterial attachment and multiplication on the surface of the medical device, thus reducing the risk of infection. Similarly, the nanopillar structures on the surface of dragonfly wings possess natural antimicrobial properties that can disrupt bacterial cell walls, preventing bacterial attachment and growth.[172] Utilizing these structures in urinary catheters and other medical devices can significantly reduce the risk of bacterial infection and improve patient safety (**Figure 12b**). Additionally, nanopillar structures enhance the mechanical strength and durability of materials, making them suitable for medical devices requiring high strength and abrasion resistance, such as long-term implanted catheters and stents. These structures also promote cell attachment and growth, improving the biocompatibility of medical devices, reducing rejection and inflammatory reactions, and enhancing the long-term efficacy of implants. Therefore, urinary catheters and other medical devices with the biological characteristics of lotus leaves and dragonflies can be fabricated using bioprinting. Urinary catheters with a lotus leaf papillary structure offer self-cleaning and low-friction advantages, reducing the risk of bacterial infection and urine scaling, and providing higher levels of comfort and safety. Catheters with a dragonfly surface nanopillar structure exhibit excellent antimicrobial properties and biocompatibility, making them suitable for long-term implantation and use. Additionally, the lotus leaf papillae and dragonfly nanopillar structures can be applied to instruments such as scalpels and forceps to improve their antifouling and antimicrobial properties, reducing the risk of postoperative infection.

Microstructures on the surface of butterfly wings hold great potential for 3D printing of ophthalmic implants and retinal repair (**Figure 12c**). These microstructures can effectively capture and manipulate light, a property that can be leveraged to design efficient optical components. When applied to retinal repair materials, they can improve the efficiency of capturing light signals and enhance the response of retinal cells to light.[173] Additionally, these microstructures can reduce light reflection and glare, improving the visual effect of ophthalmic implants and enhancing the quality of patients' vision. Furthermore, the microstructures of butterfly wings can promote cell attachment and growth, aiding in the growth and repair of retinal cells on the implant and enhancing the biocompatibility of retinal repair materials. This integration helps the implant merge better with surrounding tissues, reduces rejection, and promotes retinal regeneration and repair. Artificial retinas utilizing butterfly wing microstructures can improve the efficiency of light signal capture and conduction, enhancing the transmission of visual signals. As 3D printing technology and material science advance, the application of butterfly wing microstructures in ophthalmic implants and retinal repair will continue to expand.

The microstructure on the surface of fish scales has natural antimicrobial properties that can effectively inhibit bacterial attachment and growth. Applying this property to gastrointestinal stents can significantly reduce the risk of postoperative infection and improve the safety and reliability of the implant (**Figure 12d**). Firstly, the fish scale structure can mimic the microenvironment of natural tissues, aiding in the integration of the scaffold with gastrointestinal tract tissues, reducing the body's rejection of the scaffold, and enhancing its performance. Secondly, the unique arrangement of the fish scale structure can enhance the

mechanical properties of the scaffold, providing sufficient support and flexibility to adapt to the complex motions of the gastrointestinal tract. This structure also reduces the weight of the stent, improving patient comfort. Additionally, the micro- and nanostructures on the surface of the fish scale structure can promote cell attachment and proliferation, aiding in the rapid repair and regeneration of gastrointestinal tract tissues, thus accelerating postoperative recovery. After gastrointestinal tumor resection surgery, bioprinted scaffolds with a fish scale structure can provide stable support and promote tissue regeneration and repair.

The microstructure of the nepenthes surface has excellent liquid-guiding and self-cleaning capabilities,[126,148] effectively preventing the adhesion of bacteria and food debris on the surface of teeth. When applied to dental implants, this property significantly reduces the risk of bacterial infection and periodontal disease, extending the service life of dental implants (**Figure 12e**). The nepenthes microstructure can mimic the surface properties of natural tissues, promoting a strong bond between the dental implant and the hard and soft tissues of the oral cavity, reducing foreign body sensation and rejection. Additionally, introducing these microstructures on dental implants can promote the attachment and proliferation of bone cells, accelerating the process of osseointegration and improving the stability and success rate of dental implants. This is particularly beneficial for patients requiring bone regeneration for implantation. These microstructures also aid in the attachment and repair of gingiva and other oral soft tissues, improving the health of tissues surrounding dental implants and reducing inflammation and other complications. When applied to crowns, bridges, and other restorations, they help reduce surface staining and bacterial buildup, maintaining oral hygiene. The liquid-guided microstructure of the nepenthes demonstrates promising applications in the field of 3D-printed dental implants and oral prosthetics. This structure not only optimizes liquid guidance and antifouling properties but also enhances the biocompatibility, mechanical properties, and cell adhesion of the material, providing an innovative solution for oral healthcare.

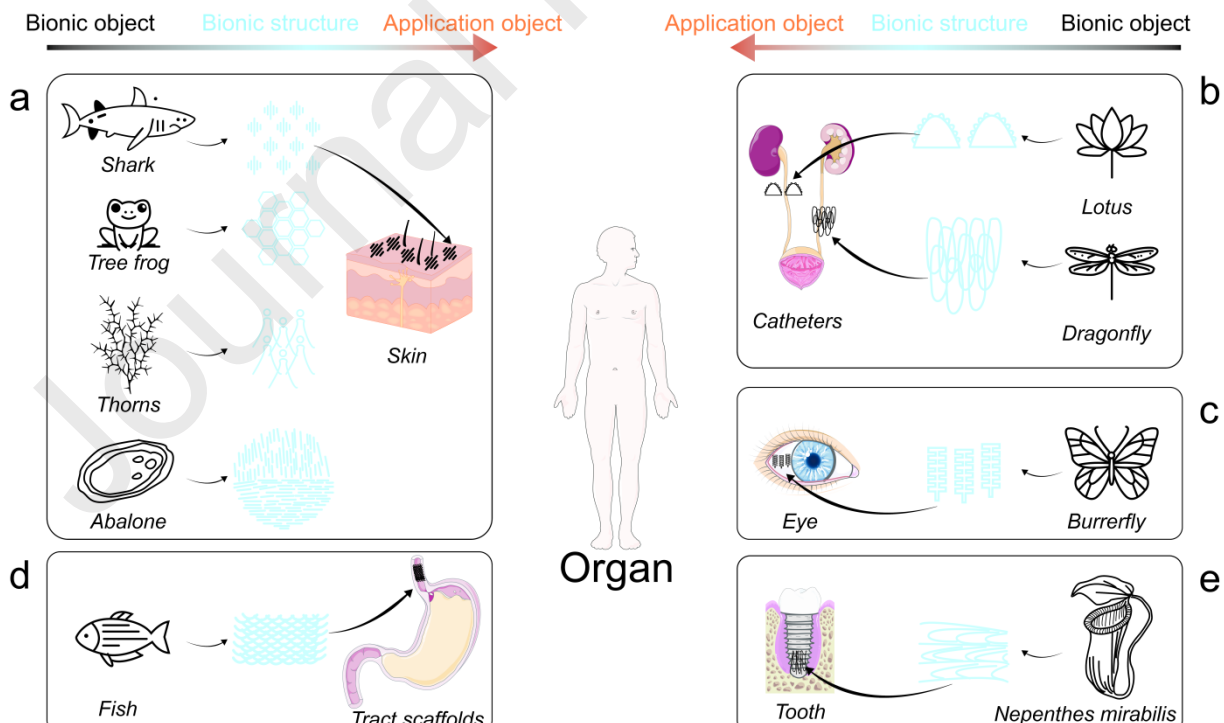


**Figure 12.** Prospective scenarios for the applicability of surface texturing in the human organs. a) Drag reduction, anti-wear, and adhesive surfaces find applications on human skin. b) Self-cleaning and antimicrobial surfaces are implemented in built-in catheters or scaffolds.

c) Optically-reflective surfaces aid in repairing visually-impaired retinas. d) Fish scale-inspired antimicrobial and anti-bio-adhesive surfaces are utilized for gastrointestinal tract scaffolds. e) Liquid-directed surfaces are used for dental implants to promote rapid healing.

#### 4.2. Surface textures in human tissues

The porous structure of sponges exhibits excellent adsorption properties, and mimicking this structure in artificial joints can enhance their mechanical properties and compatibility with the human body.[174] The integration of implants is improved by replicating the porosity and mechanical properties of natural bone, which helps to improve the biocompatibility and mechanical stability of artificial joints (**Figure 13a**). The porous structure reduces the weight of the material while providing sufficient mechanical strength to support normal joint function. It also provides space for bone cells to attach and grow, aiding in better integration at the bone-implant interface and enhancing the long-term stability and durability of the artificial joint. Bioprinting technology allows for the customization of artificial joints to match the specific needs and anatomy of the patient. By designing a specific sponge-like porous structure, implants can be optimized for individual differences among patients, improving surgical outcomes and patient comfort. The porous structure enhances the efficiency of nutrient and waste transfer between bone cells, improves metabolism, and promotes tissue repair and regeneration. Additionally, because the porous structure can better integrate with host bone tissue, it reduces the risk of implant rejection by the immune system, thereby lowering the incidence of postoperative complications. For example, knee implants with porous structural surfaces can better mimic the elasticity and strength of natural bone, helping to restore patients' motor function.

The hydrophobic hair surface structure of ants and the surface microstructure of gecko foot pads offer numerous innovations and advantages in the 3D printing cardiovascular field. The hydrophobic hair structure of ants exhibits excellent hydrophobicity, preventing liquids from remaining on its surface.[175] When applied to vascular scaffolds, this structure can significantly reduce blood retention on the scaffold surface, thereby decreasing the risk of thrombosis. The hydrophobic surface reduces the attachment of platelets and other blood components, minimizing the chances of thrombosis and inflammatory reactions on the stent surface and improving its biocompatibility. Additionally, the hydrophobic structure prevents the attachment and propagation of bacteria on the stent surface, reducing the risk of infection, which is especially crucial for cardiovascular stents implanted for long periods. The microstructure of gecko foot pads, known for its strong adhesion capacity, can form robust attachments on various surfaces (**Figure 13b**).[127] In cardiovascular applications, this can enhance the stability of vascular stents or other implants in the body, preventing migration. The gecko foot pad microstructure also promotes the attachment and growth of tissue cells, facilitating a strong integration between the scaffold and the vessel wall, thus enhancing the long-term stability and functionality of the implant. In the future, with advancements in 3D printing technology and biomaterials science, the application of ant hydrophobic hair structures and gecko foot pad microstructures in the cardiovascular field will become more extensive and in-depth.

The adhesive surface structure of spider silk holds great potential for application in the field of 3D-printed nerve repair materials (**Figure 13c**). Spider silk has special adhesive structures that effectively promote cell attachment, which can help nerve cells adhere better to repair materials and promote nerve regeneration.[176] The nanostructures on the surface of spider silk not only enhance cell attachment but also guide the direction of cell growth. In

nerve repair, this guidance helps nerve fibers grow in the intended direction, speeding up the repair process and improving the recovery of nerve function. Additionally, spider silk has excellent mechanical properties, and its surface structure can enhance the mechanical strength and flexibility of 3D-printed materials. This is crucial for nerve repair materials that need to be implanted for long periods and subjected to physiological stress. The controlled release of growth factors, anti-inflammatory drugs, and other therapeutic agents can be achieved by incorporating drug carriers into the spider silk structure. This feature provides continuous drug support in nerve repair, promoting nerve regeneration and reducing inflammatory responses. In the future, 3D-printed nerve scaffolds could adopt a spider silk surface structure to enhance the biocompatibility and mechanical properties of the scaffolds, providing a stable support environment and promoting the growth and connection of nerve fibers. This advancement in nerve repair technology has the potential to improve the quality of life for patients significantly.

The octopus sucker structure possesses extremely strong adhesion capacity, a property that can be leveraged to design 3D-printed soft tissue repair materials (**Figure 13d**). These materials can better adhere to the target tissue during the repair process, providing stable support and preventing dislocation.[177,178] Additionally, the surface of the octopus sucker has a micro- and nanoscale structure that promotes cell attachment and proliferation. This characteristic can help the repair material integrate more effectively with host tissue, accelerating tissue regeneration and repair. The octopus sucker structure not only offers adhesion but also provides flexibility and strength. This is especially important for soft tissue repair materials that need to adapt to human movement, providing the necessary support and flexibility. 3D-printed skin repair materials with an octopus sucker structure can ensure strong adhesion to skin wounds, promoting wound healing. In muscle and ligament repair, the octopus sucker structure can provide both strong adhesion and flexibility, helping the repair material integrate better and offer the necessary support to promote tissue healing and regeneration.

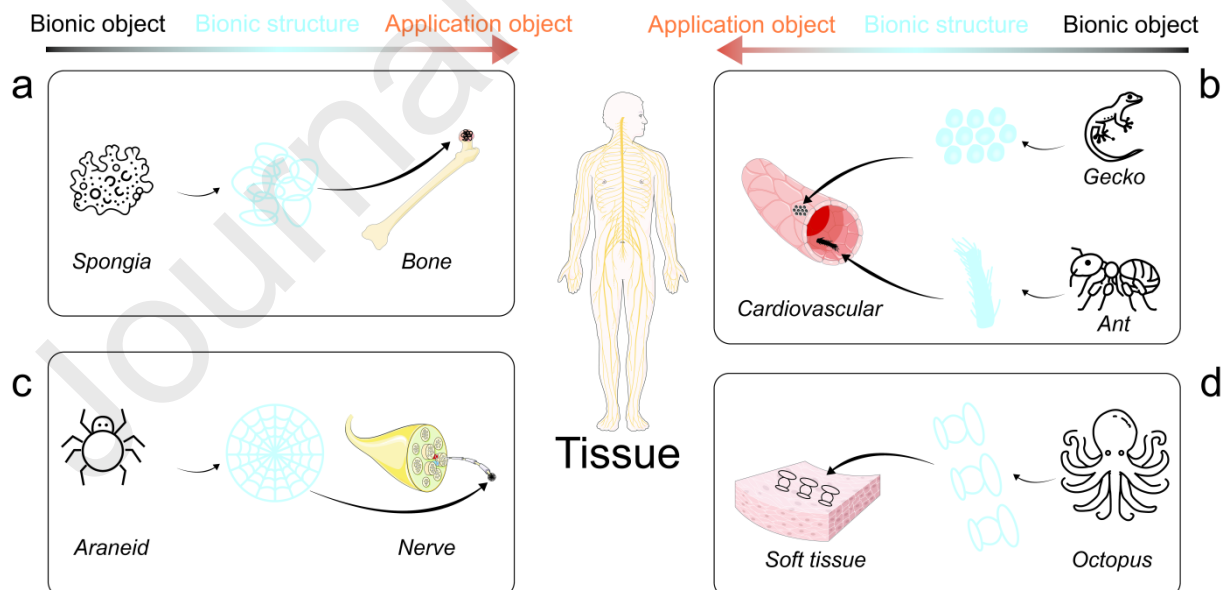


**Figure 13.** Prospective scenarios for the applicability of surface texturing in the human tissues. a) Porous structures serve as surfaces for bone or joint implants. b) Hydrophobic surfaces reduce protein and bacterial adhesion in cardiovascular implants. c) Adhesive surfaces are employed for nerve repairs. d) Adhesive surfaces support soft tissue repair and regeneration.

## 5. Perspective

With the continuous progress of 3D printing technology and material science, the application of 3D-printed bionic surfaces in biomedical engineering holds significant promise. Future advancements in 3D printing will lead to higher precision and resolution, allowing for the accurate replication of complex micro- and nanostructures found in nature. These advancements will make the application of bionic surfaces in biomedicine more extensive and effective. For instance, in fabricating vascular stents and heart valves, precise control over the size and arrangement of microstructures can enhance anti-thrombotic properties and mechanical stability. Future bionic surfaces will evolve beyond single-function capabilities to multifunctional composites. By integrating bionic surfaces with antimicrobial materials and drug release systems, biomedical devices with multiple functions can be developed. These multifunctional materials can automatically release antimicrobial drugs or growth factors post-implantation, further improving therapeutic efficacy and safety. Combining smart materials with bionic structures will enable more precise and personalized medical solutions. One key advantage of 3D printing technology is its ability to personalize. In the future, customized design and manufacturing of biomimetic surface biomedical devices will become a reality, tailored to patient-specific conditions and needs. For example, orthopedic implants and soft tissue repair materials can be designed according to a patient's anatomical structure and biomechanical requirements, enhancing surgical success rates and patient recovery.

Although bionic surfaces have shown excellent performance in the laboratory, their clinical application requires extensive validation and trials. Future efforts will focus on validating the safety and efficacy of bionic surfaces through multi-center clinical trials and large-scale studies, which will be crucial for their clinical adoption. Despite the promising results demonstrated by bionic surfaces in controlled laboratory environments, the transition to clinical application presents numerous challenges that necessitate rigorous and comprehensive validation processes. Extensive preclinical studies are imperative to establish the biocompatibility, stability, and functional performance of these surfaces under physiological conditions. Multi-center clinical trials will play a pivotal role in providing robust evidence regarding the safety and therapeutic efficacy of bionic surfaces across diverse patient populations and clinical settings.

In summary, the application of 3D-printed bionic surfaces in biomedical engineering will continue to expand and deepen. Through refined design and manufacturing, development of multifunctional composites, personalized customization, clinical validation, and multidisciplinary collaboration, bionic surfaces will drive innovation and breakthroughs in biomedical engineering, providing patients with superior medical solutions. With ongoing technological advancements, 3D-printed bionic surfaces are poised to become a vital force in the development of biomedical engineering.

## Acknowledgement

Z. M gratefully acknowledge the support of Xi'an Jiaotong University Innovative Leading Talents.

## Conflict of Interest

The authors declare no conflict of interest.

## Biographies



**Zeyu Ma** received the B.S. degree in Anhui University of Technology, Maanshan, China, in 2017 and the M.S. degree in Dalian Maritime University, Dalian, China, in 2021. He is currently a PhD candidate with School of Mechanical Engineering, Xi'an Jiaotong University and is also jointly supervised at Purdue University. His research includes bio-inspired functional surfaces, 3D printing, and flexible soft materials.



**Alex Chortos** completed his B.A.Sc in nanotechnology engineering at the University of Waterloo in 2011 and Ph.D. at Stanford University in 2017 under the guidance of Zhenan Bao. After finishing his postdoctoral fellow at Harvard University in 2020, he is currently an assistant professor at Purdue University. His research background includes bio-inspired tactile sensors, stretchable circuits, and soft actuators. His lab leverages the capabilities of 3D printing combined with materials design to pursue new device strategies for bio-integrated electronics.

## References

- [1] M.A. Skylar-Scott, J.Y. Huang, A. Lu, A.H.M. Ng, T. Duenki, S. Liu, L.L. Nam, S. Damaraju, G.M. Church, J.A. Lewis, Orthogonally induced differentiation of stem cells for the programmatic patterning of vascularized organoids and bioprinted tissues, *Nat. Biomed. Eng.* 6 (2022) 449–462. <https://doi.org/10.1038/s41551-022-00856-8>.
- [2] P. Diloksumpan, R.V. Bolaños, S. Cokelaere, B. Pouran, J. De Grauw, M. Van Rijen, R. Van Weeren, R. Levato, J. Malda, Orthotopic Bone Regeneration within 3D Printed Bioceramic Scaffolds with Region-Dependent Porosity Gradients in an Equine Model, *Adv. Healthc. Mater.* 9 (2020) 1901807. <https://doi.org/10.1002/adhm.201901807>.

- [3] M. Xie, Y. Shi, C. Zhang, M. Ge, J. Zhang, Z. Chen, J. Fu, Z. Xie, Y. He, In situ 3D bioprinting with bioconcrete bioink, *Nat. Commun.* 13 (2022) 3597. <https://doi.org/10.1038/s41467-022-30997-y>.
- [4] D. Kang, G. Hong, S. An, I. Jang, W.-S. Yun, J.-H. Shim, S. Jin, Bioprinting of Multiscaled Hepatic Lobules within a Highly Vascularized Construct, *Small* 16 (2020) 1905505. <https://doi.org/10.1002/smll.201905505>.
- [5] S.R. Moxon, M.E. Cooke, S.C. Cox, M. Snow, L. Jeys, S.W. Jones, A.M. Smith, L.M. Grover, Suspended Manufacture of Biological Structures, *Adv. Mater.* 29 (2017) 1605594. <https://doi.org/10.1002/adma.201605594>.
- [6] J. Snyder, A.R. Son, Q. Hamid, H. Wu, W. Sun, Hetero-cellular prototyping by synchronized multi-material bioprinting for rotary cell culture system, *Biofabrication* 8 (2016) 015002. <https://doi.org/10.1088/1758-5090/8/1/015002>.
- [7] A.M. Duraj-Thatte, A. Manjula-Basavanna, J. Rutledge, J. Xia, S. Hassan, A. Sourlis, A.G. Rubio, A. Lesha, M. Zenkl, A. Kan, D.A. Weitz, Y.S. Zhang, N.S. Joshi, Programmable microbial ink for 3D printing of living materials produced from genetically engineered protein nanofibers, *Nat. Commun.* 12 (2021) 6600. <https://doi.org/10.1038/s41467-021-26791-x>.
- [8] S. Choi, K.Y. Lee, S.L. Kim, L.A. MacQueen, H. Chang, J.F. Zimmerman, Q. Jin, M.M. Peters, H.A.M. Ardoña, X. Liu, A.-C. Heiler, R. Gabardi, C. Richardson, W.T. Pu, A.R. Bausch, K.K. Parker, Fibre-infused gel scaffolds guide cardiomyocyte alignment in 3D-printed ventricles, *Nat. Mater.* 22 (2023) 1039–1046. <https://doi.org/10.1038/s41563-023-01611-3>.
- [9] P.N. Bernal, M. Bouwmeester, J. Madrid-Wolff, M. Falandt, S. Florczak, N.G. Rodriguez, Y. Li, G. Größbacher, R. Samsom, M. Van Wolferen, L.J.W. Van Der Laan, P. Delrot, D. Loterie, J. Malda, C. Moser, B. Spee, R. Levato, Volumetric Bioprinting of Organoids and Optically Tuned Hydrogels to Build Liver-Like Metabolic Biofactories, *Adv. Mater.* 34 (2022) 2110054. <https://doi.org/10.1002/adma.202110054>.
- [10] D. Ribezzi, M. Gueye, S. Florczak, F. Dusi, D. De Vos, F. Manente, A. Hierholzer, M. Fussenegger, M. Caiazzo, T. Blunk, J. Malda, R. Levato, Shaping Synthetic Multicellular and Complex Multimaterial Tissues via Embedded Extrusion-Volumetric Printing of Microgels, *Adv. Mater.* 35 (2023) 2301673. <https://doi.org/10.1002/adma.202301673>.
- [11] J.A. Lewis, Direct Ink Writing of 3D Functional Materials, *Adv. Funct. Mater.* 16 (2006) 2193–2204. <https://doi.org/10.1002/adfm.200600434>.
- [12] A. Shahzad, I. Lazoglu, Direct ink writing (DIW) of structural and functional ceramics: Recent achievements and future challenges, *Compos. Part B Eng.* 225 (2021) 109249. <https://doi.org/10.1016/j.compositesb.2021.109249>.
- [13] N. Golafshan, E. Vorndran, S. Zaharievski, H. Brommer, F.B. Kadumudi, A. Dolatshahi-Pirouz, U. Gbureck, R. Van Weeren, M. Castilho, J. Malda, Tough magnesium phosphate-based 3D-printed implants induce bone regeneration in an

- equine defect model, *Biomaterials* 261 (2020) 120302.  
<https://doi.org/10.1016/j.biomaterials.2020.120302>.
- [14] R. Levato, W.R. Webb, I.A. Otto, A. Mensinga, Y. Zhang, M. Van Rijen, R. Van Weeren, I.M. Khan, J. Malda, The bio in the ink: cartilage regeneration with bioprintable hydrogels and articular cartilage-derived progenitor cells, *Acta Biomater.* 61 (2017) 41–53. <https://doi.org/10.1016/j.actbio.2017.08.005>.
- [15] N. Dubey, J.A. Ferreira, J. Malda, S.B. Bhaduri, M.C. Bottino, Extracellular Matrix/Amorphous Magnesium Phosphate Bioink for 3D Bioprinting of Craniomaxillofacial Bone Tissue, *ACS Appl. Mater. Interfaces* 12 (2020) 23752–23763. <https://doi.org/10.1021/acsami.0c05311>.
- [16] E. Shang, G. Li, Z. Zhao, N. Zhang, D. Fan, Y. Liu, Laser-Assisted Direct Ink Writing for High-Fidelity Fabrication of Elastomeric Complex Structures, *Adv. Mater. Interfaces* 10 (2023) 2300300. <https://doi.org/10.1002/admi.202300300>.
- [17] C. Dou, V. Perez, J. Qu, A. Tsin, B. Xu, J. Li, A State-of-the-Art Review of Laser-Assisted Bioprinting and its Future Research Trends, *ChemBioEng Rev.* 8 (2021) 517–534. <https://doi.org/10.1002/cben.202000037>.
- [18] S.S. Mahdavi, M.J. Abdekhodaie, H. Kumar, S. Mashayekhan, A. Baradaran-Rafii, K. Kim, Stereolithography 3D Bioprinting Method for Fabrication of Human Corneal Stroma Equivalent, *Ann. Biomed. Eng.* 48 (2020) 1955–1970.  
<https://doi.org/10.1007/s10439-020-02537-6>.
- [19] L. Elomaa, E. Keshi, I.M. Sauer, M. Weinhart, Development of GelMA/PCL and dECM/PCL resins for 3D printing of acellular in vitro tissue scaffolds by stereolithography, *Mater. Sci. Eng. C* 112 (2020) 110958.  
<https://doi.org/10.1016/j.msec.2020.110958>.
- [20] M. Taale, B. Schamberger, F. Taheri, Y. Antonelli, A. Leal-Egaña, C. Selhuber-Unkel, In Situ Fabrication of Constraints for Multicellular Micro-Spheroids Using Two-Photon Lithography, *Adv. Funct. Mater.* (2023) 2302356.  
<https://doi.org/10.1002/adfm.202302356>.
- [21] M. Tallarico, N. Baldini, F. Gatti, M. Martinolli, E. Xhanari, S.M. Meloni, C. Gabriele, L.A. Immacolata, Role of New Hydrophilic Surfaces on Early Success Rate and Implant Stability: 1-Year Post-loading Results of a Multicenter, Split-Mouth, Randomized Controlled Trial, *Eur. J. Dent.* 15 (2021) 001–007.  
<https://doi.org/10.1055/s-0040-1713952>.
- [22] C.B. Dayan, S. Chun, N. Krishna-Subbaiah, D. Drotlef, M.B. Akolpoglu, M. Sitti, 3D Printing of Elastomeric Bioinspired Complex Adhesive Microstructures, *Adv. Mater.* 33 (2021) 2103826. <https://doi.org/10.1002/adma.202103826>.
- [23] K.-M. Lee, H. Park, J. Kim, D.-M. Chun, Fabrication of a superhydrophobic surface using a fused deposition modeling (FDM) 3D printer with poly lactic acid (PLA) filament and dip coating with silica nanoparticles, *Appl. Surf. Sci.* 467–468 (2019) 979–991. <https://doi.org/10.1016/j.apsusc.2018.10.205>.
- [24] L. Wang, B. Shi, H. Zhao, X. Qi, J. Chen, J. Li, Y. Shang, K.K. Fu, X. Zhang, M. Tian, L. Qu, 3D-Printed Parahydrophobic Functional Textile with a Hierarchical

Nanomicroscale Structure, ACS Nano 16 (2022) 16645–16654.  
<https://doi.org/10.1021/acsnano.2c06069>.

- [25] Y. Zhao, X. Yang, Z. Cheng, C.H. Lau, J. Ma, L. Shao, Surface manipulation for prevention of migratory viscous crude oil fouling in superhydrophilic membranes, *Nat. Commun.* 14 (2023) 2679. <https://doi.org/10.1038/s41467-023-38419-3>.
- [26] Z. Ma, S. Lu, Y. Wu, X. Zhang, Y. Wei, F.J. Mawignon, L. Qin, L. Shan, Pressure-Activatable Liquid Metal Composites Flexible Sensor with Antifouling and Drag Reduction Functional Surface, *ACS Appl. Mater. Interfaces* 15 (2023) 54952–54965. <https://doi.org/10.1021/acsmi.3c12910>.
- [27] F. Hizal, N. Rungraeng, J. Lee, S. Jun, H.J. Busscher, H.C. Van Der Mei, C.-H. Choi, Nanoengineered Superhydrophobic Surfaces of Aluminum with Extremely Low Bacterial Adhesivity, *ACS Appl. Mater. Interfaces* 9 (2017) 12118–12129. <https://doi.org/10.1021/acsmi.7b01322>.
- [28] X. Zhang, L. Wang, E. Levänen, Superhydrophobic surfaces for the reduction of bacterial adhesion, *RSC Adv.* 3 (2013) 12003. <https://doi.org/10.1039/c3ra40497h>.
- [29] X. Liu, H. Gu, M. Wang, X. Du, B. Gao, A. Elbaz, L. Sun, J. Liao, P. Xiao, Z. Gu, 3D Printing of Bioinspired Liquid Superrepellent Structures, *Adv. Mater.* 30 (2018) 1800103. <https://doi.org/10.1002/adma.201800103>.
- [30] Y. Yamauchi, M. Tenjimbayashi, S. Samitsu, M. Naito, Durable and Flexible Superhydrophobic Materials: Abrasion/Scratching/Slicing/Droplet Impacting/Bending/Twisting-Tolerant Composite with Porcupinefish-Like Structure, *ACS Appl. Mater. Interfaces* 11 (2019) 32381–32389. <https://doi.org/10.1021/acsmi.9b09524>.
- [31] Z. Ma, X. Zhang, S. Lu, H. Yang, X. Huang, L. Qin, G. Dong, Tribological properties of flexible composite surfaces through direct ink writing for durable wearing devices, *Surf. Coat. Technol.* 441 (2022) 128573. <https://doi.org/10.1016/j.surfcoat.2022.128573>.
- [32] Q. He, Y. Zeng, L. Jiang, Z. Wang, G. Lu, H. Kang, P. Li, B. Bethers, S. Feng, L. Sun, P. Sun, C. Gong, J. Jin, Y. Hou, R. Jiang, W. Xu, E. Olevsky, Y. Yang, Growing recyclable and healable piezoelectric composites in 3D printed bioinspired structure for protective wearable sensor, *Nat. Commun.* 14 (2023) 6477. <https://doi.org/10.1038/s41467-023-41740-6>.
- [33] D.J. da Silva, A. Duran, A.D. Cabral, F.L.A. Fonseca, S.H. Wang, D.F. Parra, R.F. Bueno, I. Pereyra, D.S. Rosa, Bioinspired Antimicrobial PLA with Nanocones on the Surface for Rapid Deactivation of Omicron SARS-CoV-2, *ACS Biomater. Sci. Eng.* 9 (2023) 1891–1899. <https://doi.org/10.1021/acsbiomaterials.2c01529>.
- [34] M. Zhou, L. Zhang, L. Zhong, M. Chen, L. Zhu, T. Zhang, X. Han, Y. Hou, Y. Zheng, Robust Photothermal Icephobic Surface with Mechanical Durability of Multi-Bioinspired Structures, *Adv. Mater.* 36 (2024) 2305322. <https://doi.org/10.1002/adma.202305322>.

- [35] J. He, Q. Zhang, Y. Zhou, Y. Chen, H. Ge, S. Tang, Bioinspired Polymer Films with Surface Ordered Pyramid Arrays and 3D Hierarchical Pores for Enhanced Passive Radiative Cooling, ACS Nano (2024). <https://doi.org/10.1021/acsnano.3c12244>.
- [36] K.B. Ramadi, J.C. McRae, G. Selsing, A. Su, R. Fernandes, M. Hickling, B. Rios, S. Babaee, S. Min, D. Gwynne, N.Z. Jia, A. Aragon, K. Ishida, J. Kuosmanen, J. Jenkins, A. Hayward, K. Kamrin, G. Traverso, Bioinspired, ingestible electroceutical capsules for hunger-regulating hormone modulation, Sci. Robot. 8 (2023) eade9676. <https://doi.org/10.1126/scirobotics.ade9676>.
- [37] P. Wang, T. Zhao, R. Bian, G. Wang, H. Liu, Robust Superhydrophobic Carbon Nanotube Film with Lotus Leaf Mimetic Multiscale Hierarchical Structures, ACS Nano 11 (2017) 12385–12391. <https://doi.org/10.1021/acsnano.7b06371>.
- [38] X. Li, J. Wang, G. Yi, S.P. Teong, S.P. Chan, Y. Zhang, From waste plastic to artificial lotus leaf: Upcycling waste polypropylene to superhydrophobic spheres with hierarchical micro/nanostructure, Appl. Catal. B Environ. 342 (2024) 123378. <https://doi.org/10.1016/j.apcatb.2023.123378>.
- [39] W. Zhang, C. Hu, C. Bai, X. Zhang, S. Zhang, J. Tang, Y. Kong, T. Li, A rapid two-step process to prepare a high-throughput, efficient, reusable superhydrophobic–superoleophilic stainless steel mesh for oil/water separation, J. Adhes. Sci. Technol. (2024) 1–27. <https://doi.org/10.1080/01694243.2024.2307205>.
- [40] T. Ishizaki, N. Saito, O. Takai, Correlation of Cell Adhesive Behaviors on Superhydrophobic, Superhydrophilic, and Micropatterned Superhydrophobic/Superhydrophilic Surfaces to Their Surface Chemistry, Langmuir 26 (2010) 8147–8154. <https://doi.org/10.1021/la904447c>.
- [41] I. Hejazi, J. Seyfi, E. Hejazi, G.M.M. Sadeghi, S.H. Jafari, H.A. Khonakdar, Investigating the role of surface micro/nano structure in cell adhesion behavior of superhydrophobic polypropylene/nanosilica surfaces, Colloids Surf. B Biointerfaces 127 (2015) 233–240. <https://doi.org/10.1016/j.colsurfb.2015.01.054>.
- [42] N. Chokesawatanakit, S. Thammasang, S. Phanthanawiboon, J.T.N. Knijnenburg, S. Theerakulpisut, K. Kamwilaisak, Enhancing the multifunctional properties of cellulose fabrics through *in situ* hydrothermal deposition of TiO<sub>2</sub> nanoparticles at low temperature for antibacterial self-cleaning under UV–Vis illumination, Int. J. Biol. Macromol. 256 (2024) 128321. <https://doi.org/10.1016/j.ijbiomac.2023.128321>.
- [43] A.A. Abraham, A.K. Means, F.J.Jr. Clubb, R. Fei, A.K. Locke, E.G. Gacasan, G.L. Coté, M.A. Grunlan, Foreign Body Reaction to a Subcutaneously Implanted Self-Cleaning, Thermoresponsive Hydrogel Membrane for Glucose Biosensors, ACS Biomater. Sci. Eng. 4 (2018) 4104–4111. <https://doi.org/10.1021/acsbiomaterials.8b01061>.
- [44] S.H. Ku, J. Ryu, S.K. Hong, H. Lee, C.B. Park, General functionalization route for cell adhesion on non-wetting surfaces, Biomaterials 31 (2010) 2535–2541. <https://doi.org/10.1016/j.biomaterials.2009.12.020>.

- [45] H. Matsumura, M. Saburi, Protein adsorption and wetting of the protein adsorbed surfaces studied by a new type of laser reflectometer, *Colloids Surf. B Biointerfaces* 47 (2006) 146–152. <https://doi.org/10.1016/j.colsurfb.2005.12.004>.
- [46] Z. Ma, J. Liu, X. Zhang, R. Deng, S. Lu, Y. Wu, L. Qin, G. Dong, Flexible surfaces prepared through direct ink writing with drag reduction and antifouling, *Colloids Surf. Physicochem. Eng. Asp.* 655 (2022) 130233. <https://doi.org/10.1016/j.colsurfa.2022.130233>.
- [47] J. Marlena, J.K.S. Tan, Z. Lin, D.X. Li, B. Zhao, H.L. Leo, S. Kim, C.H. Yap, Monolithic polymeric porous superhydrophobic material with pneumatic plastron stabilization for functionally durable drag reduction in blood-contacting biomedical applications, *NPG Asia Mater.* 13 (2021) 1–12. <https://doi.org/10.1038/s41427-021-00325-9>.
- [48] J.K.S. Tan, E.S.A. Chen, Y. Dong, H. Fang, C.Y. Koh, R.M. Kini, S. Kim, H.L. Leo, C.H. Yap, Antithrombotic and Flow Drag-Reducing Material for Blood-Contacting Medical Devices, *Adv. Mater. Interfaces* 10 (2023) 2202270. <https://doi.org/10.1002/admi.202202270>.
- [49] J. Warner, P. Soman, W. Zhu, M. Tom, S. Chen, Design and 3D Printing of Hydrogel Scaffolds with Fractal Geometries, *ACS Biomater. Sci. Eng.* 2 (2016) 1763–1770. <https://doi.org/10.1021/acsbiomaterials.6b00140>.
- [50] L. Zhang, X. He, W. He, S. Zhang, M. Zhao, H. Zhao, High maneuverability of the falcon flying robot, *J. Field Robot.* 41 (2024) 539–549. <https://doi.org/10.1002/rob.22277>.
- [51] Y. Zhang, H. Wu, J. Zhao, S. Yan, Design and performance analysis of morphing nose cone driven by a novel bionic parallel mechanism for aerospace vehicle, *Aerospace Sci. Technol.* 139 (2023) 108365. <https://doi.org/10.1016/j.ast.2023.108365>.
- [52] L. Qin, Z. Ma, H. Sun, S. Lu, Q. Zeng, Y. Zhang, G. Dong, Drag reduction and antifouling properties of non-smooth surfaces modified with ZIF-67, *Surf. Coat. Technol.* 427 (2021) 127836. <https://doi.org/10.1016/j.surfcoat.2021.127836>.
- [53] S. Shi, Y. Ming, H. Wu, C. Zhi, L. Yang, S. Meng, Y. Si, D. Wang, B. Fei, J. Hu, A Bionic Skin for Health Management: Excellent Breathability, In Situ Sensing, and Big Data Analysis, *Adv. Mater.* 36 (2024) 2306435. <https://doi.org/10.1002/adma.202306435>.
- [54] J. Waeterschoot, W. Gosselé, Š. Lemež, X. Casadevall i Solvas, Artificial cells for in vivo biomedical applications through red blood cell biomimicry, *Nat. Commun.* 15 (2024) 2504. <https://doi.org/10.1038/s41467-024-46732-8>.
- [55] J. Yang, M. Feng, J. Wang, Z. Zhao, R. Xu, Z. Chen, K. Zhang, A. Khan, Y. Han, F. Song, W. Huang, Bionic Micro-Texture Duplication and RE3+ Space-Selective Doping of Unclonable Silica Nanocomposites for Multilevel Encryption and Intelligent Authentication, *Adv. Mater.* 35 (2023) 2306003. <https://doi.org/10.1002/adma.202306003>.

- [56] L.J. Pourchet, A. Thepot, M. Albouy, E.J. Courtial, A. Boher, L.J. Blum, C.A. Marquette, Human Skin 3D Bioprinting Using Scaffold-Free Approach, *Adv. Healthc. Mater.* 6 (2017) 1601101. <https://doi.org/10.1002/adhm.201601101>.
- [57] L. Hafa, L. Breideband, L. Ramirez Posada, N. Torras, E. Martinez, E.H.K. Stelzer, F. Pampaloni, Light Sheet-Based Laser Patterning Bioprinting Produces Long-Term Viable Full-Thickness Skin Constructs, *Adv. Mater.* 36 (2024) 2306258. <https://doi.org/10.1002/adma.202306258>.
- [58] A. Jafari, S. Vahid Niknezhad, M. Kaviani, W. Saleh, N. Wong, P.P. Van Vliet, C. Moraes, A. Ajji, L. Kadem, N. Azarpira, G. Andelfinger, H. Savoji, Formulation and Evaluation of PVA/Gelatin/Carrageenan Inks for 3D Printing and Development of Tissue-Engineered Heart Valves, *Adv. Funct. Mater.* 34 (2024) 2305188. <https://doi.org/10.1002/adfm.202305188>.
- [59] Y. Fang, Y. Guo, B. Wu, Z. Liu, M. Ye, Y. Xu, M. Ji, L. Chen, B. Lu, K. Nie, Z. Wang, J. Luo, T. Zhang, W. Sun, Z. Xiong, Expanding Embedded 3D Bioprinting Capability for Engineering Complex Organs with Freeform Vascular Networks, *Adv. Mater.* 35 (2023) 2205082. <https://doi.org/10.1002/adma.202205082>.
- [60] Z. Zhou, L. Ruiz Cantu, X. Chen, M.R. Alexander, C.J. Roberts, R. Hague, C. Tuck, D. Irvine, R. Wildman, High-throughput characterization of fluid properties to predict droplet ejection for three-dimensional inkjet printing formulations, *Addit. Manuf.* 29 (2019) 100792. <https://doi.org/10.1016/j.addma.2019.100792>.
- [61] J.H. Ahrens, S.G.M. Uzel, M. Skylar-Scott, M.M. Mata, A. Lu, K.T. Kroll, J.A. Lewis, Programming Cellular Alignment in Engineered Cardiac Tissue via Bioprinting Anisotropic Organ Building Blocks, *Adv. Mater.* 34 (2022) 2200217. <https://doi.org/10.1002/adma.202200217>.
- [62] F. Guillemot, A. Souquet, S. Catros, B. Guillotin, Laser-assisted cell printing: principle, physical parameters versus cell fate and perspectives in tissue engineering, *Nanomed.* 5 (2010) 507–515. <https://doi.org/10.2217/nnm.10.14>.
- [63] P.F. Costa, H.J. Albers, J.E.A. Linssen, H.H.T. Middelkamp, L. Van Der Hout, R. Passier, A. Van Den Berg, J. Malda, A.D. Van Der Meer, Mimicking arterial thrombosis in a 3D-printed microfluidic in vitro vascular model based on computed tomography angiography data, *Lab. Chip* 17 (2017) 2785–2792. <https://doi.org/10.1039/C7LC00202E>.
- [64] Q. Wang, Y. Liao, Y. Ho, K. Wang, W. Jin, Y. Guan, W. Fu, A study on cell viability based on thermal inkjet three-dimensional bioprinting, *Phys. Fluids* 35 (2023) 082007. <https://doi.org/10.1063/5.0159135>.
- [65] J.A. Phillipi, E. Miller, L. Weiss, J. Huard, A. Waggoner, P. Campbell, Microenvironments Engineered by Inkjet Bioprinting Spatially Direct Adult Stem Cells Toward Muscle- and Bone-Like Subpopulations, *Stem Cells* 26 (2008) 127–134. <https://doi.org/10.1634/stemcells.2007-0520>.
- [66] T. Sekitani, Y. Noguchi, U. Zschieschang, H. Klauk, T. Someya, Organic transistors manufactured using inkjet technology with subfemtoliter accuracy, *Proc. Natl. Acad. Sci.* 105 (2008) 4976–4980. <https://doi.org/10.1073/pnas.0708340105>.

- [67] M. Singh, H.M. Haverinen, P. Dhagat, G.E. Jabbour, Inkjet Printing—Process and Its Applications, *Adv. Mater.* 22 (2010) 673–685. <https://doi.org/10.1002/adma.200901141>.
- [68] U. Demirci, G. Montesano, Single cell epitaxy by acoustic picolitre droplets, *Lab. Chip* 7 (2007) 1139–1145. <https://doi.org/10.1039/B704965J>.
- [69] W. Kim, Y. Lee, D. Kang, T. Kwak, H.-R. Lee, S. Jung, 3D Inkjet-Bioprinted Lung-on-a-Chip, *ACS Biomater. Sci. Eng.* 9 (2023) 2806–2815. <https://doi.org/10.1021/acsbiomaterials.3c00089>.
- [70] J. Ji, C. Zhao, C. Hua, L. Lu, Y. Pang, W. Sun, 3D Printing Cervical Implant Scaffolds Incorporated with Drug-Loaded Carboxylated Chitosan Microspheres for Long-Term Anti-HPV Protein Delivery, *ACS Biomater. Sci. Eng.* 10 (2024) 1544–1553. <https://doi.org/10.1021/acsbiomaterials.3c01594>.
- [71] N. Golafshan, K. Willemse, F.B. Kadumudi, E. Vorndran, A. Dolatshahi-Pirouz, H. Weinans, B.C.H. Van Der Wal, J. Malda, M. Castilho, 3D-Printed Regenerative Magnesium Phosphate Implant Ensures Stability and Restoration of Hip Dysplasia, *Adv. Healthc. Mater.* 10 (2021) 2101051. <https://doi.org/10.1002/adhm.202101051>.
- [72] D.B. Kolesky, R.L. Truby, A.S. Gladman, T.A. Busbee, K.A. Homan, J.A. Lewis, 3D Bioprinting of Vascularized, Heterogeneous Cell-Laden Tissue Constructs, *Adv. Mater.* 26 (2014) 3124–3130. <https://doi.org/10.1002/adma.201305506>.
- [73] L. Ning, B. Yang, F. Mohabatpour, N. Betancourt, M.D. Sarker, P. Papagerakis, X. Chen, Process-induced cell damage: pneumatic versus screw-driven bioprinting, *Biofabrication* 12 (2020) 025011. <https://doi.org/10.1088/1758-5090/ab5f53>.
- [74] D.X.B. Chen, Extrusion Bioprinting of Scaffolds: An Introduction, in: D.X.B. Chen (Ed.), *Extrus. Bioprinting Scaffolds Tissue Eng. Appl.*, Springer International Publishing, Cham, 2019: pp. 1–13. [https://doi.org/10.1007/978-3-030-03460-3\\_1](https://doi.org/10.1007/978-3-030-03460-3_1).
- [75] G. Cedillo-Servin, O. Dahri, J. Meneses, J. Van Duijn, H. Moon, F. Sage, J. Silva, A. Pereira, F.D. Magalhães, J. Malda, N. Geijsen, A.M. Pinto, M. Castilho, 3D Printed Magneto-Active Microfiber Scaffolds for Remote Stimulation and Guided Organization of 3D In Vitro Skeletal Muscle Models, *Small* 20 (2024) 2307178. <https://doi.org/10.1002/smll.202307178>.
- [76] S.G.M. Uzel, R.D. Weeks, M. Eriksson, D. Kokkinis, J.A. Lewis, Multimaterial Multinozzle Adaptive 3D Printing of Soft Materials, *Adv. Mater. Technol.* 7 (2022) 2101710. <https://doi.org/10.1002/admt.202101710>.
- [77] N. Jones, Science in three dimensions: The print revolution, *Nature* 487 (2012) 22–23. <https://doi.org/10.1038/487022a>.
- [78] G. Boix-Lemonche, R.M. Nagymihaly, E.M. Niemi, N. Josifovska, S. Johansen, M.C. Moe, H. Scholz, G. Petrovski, Intracorneal Implantation of 3D Bioprinted Scaffolds Containing Mesenchymal Stromal Cells Using Femtosecond-Laser-Assisted Intrastromal Keratoplasty, *Macromol. Biosci.* 23 (2023) 2200422. <https://doi.org/10.1002/mabi.202200422>.

- [79] S. Catros, B. Guillotin, M. Bačáková, J.-C. Fricain, F. Guillemot, Effect of laser energy, substrate film thickness and bioink viscosity on viability of endothelial cells printed by Laser-Assisted Bioprinting, *Appl. Surf. Sci.* 257 (2011) 5142–5147. <https://doi.org/10.1016/j.apsusc.2010.11.049>.
- [80] S.V. Murphy, A. Atala, 3D bioprinting of tissues and organs, *Nat. Biotechnol.* 32 (2014) 773–785. <https://doi.org/10.1038/nbt.2958>.
- [81] Z. Zhang, R. Xiong, R. Mei, Y. Huang, D.B. Chrisey, Time-Resolved Imaging Study of Jetting Dynamics during Laser Printing of Viscoelastic Alginate Solutions, *Langmuir* 31 (2015) 6447–6456. <https://doi.org/10.1021/acs.langmuir.5b00919>.
- [82] B. Guillotin, A. Souquet, S. Catros, M. Duocastella, B. Pippenger, S. Bellance, R. Bareille, M. Rémy, L. Bordenave, J. Amédée, F. Guillemot, Laser assisted bioprinting of engineered tissue with high cell density and microscale organization, *Biomaterials* 31 (2010) 7250–7256. <https://doi.org/10.1016/j.biomaterials.2010.05.055>.
- [83] P. Chansoria, R. Shirwaiker, 3D bioprinting of anisotropic engineered tissue constructs with ultrasonically induced cell patterning, *Addit. Manuf.* 32 (2020) 101042. <https://doi.org/10.1016/j.addma.2020.101042>.
- [84] A. Sorkio, L. Koch, L. Koivusalo, A. Deiwick, S. Miettinen, B. Chichkov, H. Skottman, Human stem cell based corneal tissue mimicking structures using laser-assisted 3D bioprinting and functional bioinks, *Biomaterials* 171 (2018) 57–71. <https://doi.org/10.1016/j.biomaterials.2018.04.034>.
- [85] Y. Shanjani, C.C. Pan, L. Elomaa, Y. Yang, A novel bioprinting method and system for forming hybrid tissue engineering constructs, *Biofabrication* 7 (2015) 045008. <https://doi.org/10.1088/1758-5090/7/4/045008>.
- [86] Z. Wang, H. Kumar, Z. Tian, X. Jin, J.F. Holzman, F. Menard, K. Kim, Visible Light Photoinitiation of Cell-Adhesive Gelatin Methacryloyl Hydrogels for Stereolithography 3D Bioprinting, *ACS Appl. Mater. Interfaces* 10 (2018) 26859–26869. <https://doi.org/10.1021/acsami.8b06607>.
- [87] B. Zhang, X. Gui, P. Song, X. Xu, L. Guo, Y. Han, L. Wang, C. Zhou, Y. Fan, X. Zhang, Three-Dimensional Printing of Large-Scale, High-Resolution Bioceramics with Micronano Inner Porosity and Customized Surface Characterization Design for Bone Regeneration, *ACS Appl. Mater. Interfaces* 14 (2022) 8804–8815. <https://doi.org/10.1021/acsami.1c22868>.
- [88] X. Kuang, J. Wu, K. Chen, Z. Zhao, Z. Ding, F. Hu, D. Fang, H.J. Qi, Grayscale digital light processing 3D printing for highly functionally graded materials, *Sci. Adv.* 5 (2019) eaav5790. <https://doi.org/10.1126/sciadv.aav5790>.
- [89] Y. Chen, J. Zhang, X. Liu, S. Wang, J. Tao, Y. Huang, W. Wu, Y. Li, K. Zhou, X. Wei, S. Chen, X. Li, X. Xu, L. Cardon, Z. Qian, M. Gou, Noninvasive in vivo 3D bioprinting, *Sci. Adv.* 6 (2020) eaba7406. <https://doi.org/10.1126/sciadv.aba7406>.
- [90] S. Krainer, C. Smit, U. Hirn, The effect of viscosity and surface tension on inkjet printed picoliter dots, *RSC Adv.* 9 (2019) 31708–31719. <https://doi.org/10.1039/C9RA04993B>.

- [91] R. Bernasconi, S. Brovelli, P. Viviani, M. Soldo, D. Giusti, L. Magagnin, Piezoelectric Drop-On-Demand Inkjet Printing of High-Viscosity Inks, *Adv. Eng. Mater.* 24 (2022) 2100733. <https://doi.org/10.1002/adem.202100733>.
- [92] Z. Weng, Y. Zhou, W. Lin, T. Senthil, L. Wu, Structure-property relationship of nano enhanced stereolithography resin for desktop SLA 3D printer, *Compos. Part Appl. Sci. Manuf.* 88 (2016) 234–242. <https://doi.org/10.1016/j.compositesa.2016.05.035>.
- [93] D.M. Shah, J. Morris, T.A. Plaisted, A.V. Amirkhizi, C.J. Hansen, Highly filled resins for DLP-based printing of low density, high modulus materials, *Addit. Manuf.* 37 (2021) 101736. <https://doi.org/10.1016/j.addma.2020.101736>.
- [94] Y. Yan, X. Li, Y. Gao, S. Mathivanan, L. Kong, Y. Tao, Y. Dong, X. Li, A. Bhattacharyya, X. Zhao, S.-C. Zhang, 3D bioprinting of human neural tissues with functional connectivity, *Cell Stem Cell* 31 (2024) 260-274.e7. <https://doi.org/10.1016/j.stem.2023.12.009>.
- [95] E. M. Maines, M. K. Porwal, C. J. Ellison, T. M. Reineke, Sustainable advances in SLA/DLP 3D printing materials and processes, *Green Chem.* 23 (2021) 6863–6897. <https://doi.org/10.1039/D1GC01489G>.
- [96] S.V. Murphy, A. Skardal, A. Atala, Evaluation of hydrogels for bio-printing applications, *J. Biomed. Mater. Res. A* 101A (2013) 272–284. <https://doi.org/10.1002/jbm.a.34326>.
- [97] Y. He, Z. Gu, M. Xie, J. Fu, H. Lin, Why choose 3D bioprinting? Part II: methods and bioprinters, *Bio-Des. Manuf.* 3 (2020) 1–4. <https://doi.org/10.1007/s42242-020-00064-w>.
- [98] Y. Wang, N. Willenbacher, Phase-Change-Enabled, Rapid, High-Resolution Direct Ink Writing of Soft Silicone, *Adv. Mater.* 34 (2022) 2109240. <https://doi.org/10.1002/adma.202109240>.
- [99] N. Vidhu, A. Gupta, R. Salajeghe, J. Spangenberg, D. Marla, A computational model for stereolithography apparatus (SLA) 3D printing, *Prog. Addit. Manuf.* (2023). <https://doi.org/10.1007/s40964-023-00525-5>.
- [100] C.M. Smith, A.L. Stone, R.L. Parkhill, R.L. Stewart, M.W. Simpkins, A.M. Kachurin, W.L. Warren, S.K. Williams, Three-Dimensional BioAssembly Tool for Generating Viable Tissue-Engineered Constructs, *Tissue Eng.* 10 (2004) 1566–1576. <https://doi.org/10.1089/ten.2004.10.1566>.
- [101] T. Zandrini, S. Florczak, R. Levato, A. Ovsianikov, Breaking the resolution limits of 3D bioprinting: future opportunities and present challenges, *Trends Biotechnol.* 41 (2023) 604–614. <https://doi.org/10.1016/j.tibtech.2022.10.009>.
- [102] H. Goodarzi Hosseinabadi, E. Dogan, A.K. Miri, L. Ionov, Digital Light Processing Bioprinting Advances for Microtissue Models, *ACS Biomater. Sci. Eng.* 8 (2022) 1381–1395. <https://doi.org/10.1021/acsbiomaterials.1c01509>.
- [103] T. Xu, J. Jin, C. Gregory, J.J. Hickman, T. Boland, Inkjet printing of viable mammalian cells, *Biomaterials* 26 (2005) 93–99. <https://doi.org/10.1016/j.biomaterials.2004.04.011>.

- [104] S. Boularaoui, G. Al Hussein, K.A. Khan, N. Christoforou, C. Stefanini, An overview of extrusion-based bioprinting with a focus on induced shear stress and its effect on cell viability, *Bioprinting* 20 (2020) e00093. <https://doi.org/10.1016/j.bprint.2020.e00093>.
- [105] C. Dou, V. Perez, J. Qu, A. Tsin, B. Xu, J. Li, A State-of-the-Art Review of Laser-Assisted Bioprinting and its Future Research Trends, *ChemBioEng Rev.* 8 (2021) 517–534. <https://doi.org/10.1002/cben.202000037>.
- [106] J. Huh, Y.-W. Moon, J. Park, A. Atala, J.J. Yoo, S.J. Lee, Combinations of photoinitiator and UV absorber for cell-based digital light processing (DLP) bioprinting, *Biofabrication* 13 (2021) 034103. <https://doi.org/10.1088/1758-5090/abfd7a>.
- [107] H. Xu, Q. Liu, J. Casillas, M. Mcanally, N. Mubtasim, L.S. Gollahan, D. Wu, C. Xu, Prediction of cell viability in dynamic optical projection stereolithography-based bioprinting using machine learning, *J. Intell. Manuf.* 33 (2022) 995–1005. <https://doi.org/10.1007/s10845-020-01708-5>.
- [108] W.L. Ng, X. Huang, V. Shkolnikov, R. Suntornnond, W.Y. Yeong, Polyvinylpyrrolidone-based bioink: influence of bioink properties on printing performance and cell proliferation during inkjet-based bioprinting, *Bio-Des. Manuf.* 6 (2023) 676–690. <https://doi.org/10.1007/s42242-023-00245-3>.
- [109] F. Marga, K. Jakab, C. Khatiwala, B. Shepherd, S. Dorfman, B. Hubbard, S. Colbert, G. Forgacs, Toward engineering functional organ modules by additive manufacturing, *Biofabrication* 4 (2012) 022001. <https://doi.org/10.1088/1758-5082/4/2/022001>.
- [110] S. You, Y. Xiang, H.H. Hwang, D.B. Berry, W. Kiratitanaporn, J. Guan, E. Yao, M. Tang, Z. Zhong, X. Ma, D. Wangpraseurt, Y. Sun, T. Lu, S. Chen, High cell density and high-resolution 3D bioprinting for fabricating vascularized tissues, *Sci. Adv.* 9 (2023) eade7923. <https://doi.org/10.1126/sciadv.adc7923>.
- [111] H. Kumar, K. Kim, Stereolithography 3D Bioprinting, in: J.M. Crook (Ed.), *3D Bioprinting Princ. Protoc.*, Springer US, New York, NY, 2020: pp. 93–108. [https://doi.org/10.1007/978-1-0716-0520-2\\_6](https://doi.org/10.1007/978-1-0716-0520-2_6).
- [112] Y. Cao, J. Tan, H. Zhao, T. Deng, Y. Hu, J. Zeng, J. Li, Y. Cheng, J. Tang, Z. Hu, K. Hu, B. Xu, Z. Wang, Y. Wu, P.E. Lobie, S. Ma, Bead-jet printing enabled sparse mesenchymal stem cell patterning augments skeletal muscle and hair follicle regeneration, *Nat. Commun.* 13 (2022) 7463. <https://doi.org/10.1038/s41467-022-35183-8>.
- [113] Y. Zhao, Y. Li, S. Mao, W. Sun, R. Yao, The influence of printing parameters on cell survival rate and printability in microextrusion-based 3D cell printing technology, *Biofabrication* 7 (2015) 045002. <https://doi.org/10.1088/1758-5090/7/4/045002>.
- [114] L. Moroni, J.A. Burdick, C. Highley, S.J. Lee, Y. Morimoto, S. Takeuchi, J.J. Yoo, Biofabrication strategies for 3D in vitro models and regenerative medicine, *Nat. Rev. Mater.* 3 (2018) 21–37. <https://doi.org/10.1038/s41578-018-0006-y>.
- [115] J. Yang, F. Zhou, R. Xing, Y. Lin, Y. Han, C. Teng, Q. Wang, Development of Large-Scale Size-Controlled Adult Pancreatic Progenitor Cell Clusters by an Inkjet-Printing

Technique, ACS Appl. Mater. Interfaces 7 (2015) 11624–11630.  
<https://doi.org/10.1021/acsami.5b02676>.

- [116] M. Hospodiuk, M. Dey, D. Sosnoski, I.T. Ozbolat, The bioink: A comprehensive review on bioprintable materials, Biotechnol. Adv. 35 (2017) 217–239.  
<https://doi.org/10.1016/j.biotechadv.2016.12.006>.
- [117] S. Hewes, A.D. Wong, P.C. Searson, Bioprinting microvessels using an inkjet printer, Bioprinting 7 (2017) 14–18. <https://doi.org/10.1016/j.bprint.2017.05.002>.
- [118] A. Dufour, X.B. Gallostra, C. O'Keeffe, K. Eichholz, S. Von Euw, O. Garcia, D.J. Kelly, Integrating melt electrowriting and inkjet bioprinting for engineering structurally organized articular cartilage, Biomaterials 283 (2022) 121405.  
<https://doi.org/10.1016/j.biomaterials.2022.121405>.
- [119] 3D printer creates brain tissue that acts like the real thing, (2024).  
<https://www.science.org/content/article/3d-printer-creates-brain-tissue-acts-real-thing> (accessed May 3, 2024).
- [120] S.J. Wu, J. Wu, S.J. Kaser, H. Roh, R.D. Shiferaw, H. Yuk, X. Zhao, A 3D printable tissue adhesive, Nat. Commun. 15 (2024) 1215. <https://doi.org/10.1038/s41467-024-45147-9>.
- [121] R. Xiong, Z. Zhang, W. Chai, Y. Huang, D.B. Chrisey, Freeform drop-on-demand laser printing of 3D alginate and cellular constructs, Biofabrication 7 (2015) 045011.  
<https://doi.org/10.1088/1758-5090/7/4/045011>.
- [122] O. Kérourédan, D. Hakobyan, M. Rémy, S. Ziane, N. Dusserre, J.-C. Fricain, S. Delmond, N.B. Thébaud, R. Devillard, In situ prevascularization designed by laser-assisted bioprinting: effect on bone regeneration, Biofabrication 11 (2019) 045002.  
<https://doi.org/10.1088/1758-5090/ab2620>.
- [123] C. Qiu, Y. Sun, J. Li, J. Zhou, Y. Xu, C. Qiu, K. Yu, J. Liu, Y. Jiang, W. Cui, G. Wang, H. Liu, W. Yuan, T. Jiang, Y. Kou, Z. Ge, Z. He, S. Zhang, Y. He, L. Yu, A 3D-Printed Dual Driving Forces Scaffold with Self-Promoted Cell Absorption for Spinal Cord Injury Repair, Adv. Sci. 10 (2023) 2301639. <https://doi.org/10.1002/advs.202301639>.
- [124] S.H. Kim, Y.K. Yeon, J.M. Lee, J.R. Chao, Y.J. Lee, Y.B. Seo, M.T. Sultan, O.J. Lee, J.S. Lee, S. Yoon, I.-S. Hong, G. Khang, S.J. Lee, J.J. Yoo, C.H. Park, Precisely printable and biocompatible silk fibroin bioink for digital light processing 3D printing, Nat. Commun. 9 (2018) 1620. <https://doi.org/10.1038/s41467-018-03759-y>.
- [125] B. Grigoryan, S.J. Paulsen, D.C. Corbett, D.W. Sazer, C.L. Fortin, A.J. Zaita, P.T. Greenfield, N.J. Calafat, J.P. Gounley, A.H. Ta, F. Johansson, A. Randles, J.E. Rosenkrantz, J.D. Louis-Rosenberg, P.A. Galie, K.R. Stevens, J.S. Miller, Multivascular networks and functional intravascular topologies within biocompatible hydrogels, Science 364 (2019) 458–464. <https://doi.org/10.1126/science.aav9750>.
- [126] ‘Toxic bait’ from Indian pitcher plants lures hungry insects to their doom, (2023).  
<https://www.science.org/content/article/toxic-bait-indian-pitcher-plants-lures-hungry-insects-their-doom> (accessed May 24, 2024).

- [127] G.S. Watson, D.W. Green, L. Schwarzkopf, X. Li, B.W. Cribb, S. Myhra, J.A. Watson, A gecko skin micro/nano structure – A low adhesion, superhydrophobic, anti-wetting, self-cleaning, biocompatible, antibacterial surface, *Acta Biomater.* 21 (2015) 109–122. <https://doi.org/10.1016/j.actbio.2015.03.007>.
- [128] Z. Ma, Y. Wu, S. Lu, J. Li, J. Liu, X. Huang, X. Zhang, Y. Zhang, G. Dong, L. Qin, S. Yang, Magnetically Assisted 3D Printing of Ultra-Antiwear Flexible Sensor, *Adv. Funct. Mater.* (2024) 2406108. <https://doi.org/10.1002/adfm.202406108>.
- [129] G. Chomicki, G. Burin, L. Busta, J. Gozdzik, R. Jetter, B. Mortimer, U. Bauer, Convergence in carnivorous pitcher plants reveals a mechanism for composite trait evolution, *Science* 383 (2024) 108–113. <https://doi.org/10.1126/science.ade0529>.
- [130] C. Li, L. Jiang, J. Hu, C. Xu, Z. Li, W. Liu, X. Zhao, B. Zhao, Superhydrophilic–Superhydrophobic Multifunctional Janus Foam Fabrication Using a Spatially Shaped Femtosecond Laser for Fog Collection and Detection, *ACS Appl. Mater. Interfaces* 14 (2022) 9873–9881. <https://doi.org/10.1021/acsami.1c24284>.
- [131] K.R. Hossain, J. Wu, X. Xu, K. Cobra, M.M. Jami, M.B. Ahmed, X. Wang, Tribological bioinspired interfaces for 3D printing, *Tribol. Int.* 188 (2023) 108904. <https://doi.org/10.1016/j.triboint.2023.108904>.
- [132] Q. He, T. Tang, Y. Zeng, N. Iradukunda, B. Bethers, X. Li, Y. Yang, Review on 3D Printing of Bioinspired Structures for Surface/Interface Applications, *Adv. Funct. Mater.* 34 (2024) 2309323. <https://doi.org/10.1002/adfm.202309323>.
- [133] E. Sachs, A. Curodeau, D. Gossard, H. Jee, M. Cima, S. Caldarise, Surface Texture by 3D Printing, *Univ. Tex. Austin* (1994) 56–64.
- [134] Z. Dong, M. Vuckovac, W. Cui, Q. Zhou, R.H.A. Ras, P.A. Levkin, 3D Printing of Superhydrophobic Objects with Bulk Nanostructure, *Adv. Mater.* 33 (2021) 2106068. <https://doi.org/10.1002/adma.202106068>.
- [135] Y. Yang, X. Li, X. Zheng, Z. Chen, Q. Zhou, Y. Chen, 3D-Printed Biomimetic Super-Hydrophobic Structure for Microdroplet Manipulation and Oil/Water Separation, *Adv. Mater.* 30 (2018) 1704912. <https://doi.org/10.1002/adma.201704912>.
- [136] W. Dai, M. Alkahtani, P.R. Hemmer, H. Liang, Drag-reduction of 3D printed shark-skin-like surfaces, *Friction* 7 (2019) 603–612. <https://doi.org/10.1007/s40544-018-0246-2>.
- [137] Z. Ma, X. Zhang, H. Liu, S. Lu, L. Qin, G. Dong, Direct ink writing of reinforced polydimethylsiloxane elastomer composites for flexure sensors, *J. Appl. Polym. Sci.* 139 (2022) e53153. <https://doi.org/10.1002/app.53153>.
- [138] S. Ma, H. Yang, S. Fu, Y. Hu, P. He, Z. Sun, X. Duan, D. Jia, P. Colombo, Y. Zhou, Additive manufacturing of hierarchical Zeolite-A lattices with exceptionally high Cs<sup>+</sup> adsorption capacity and near-unity immobilization efficiency, *Chem. Eng. J.* 474 (2023) 145909. <https://doi.org/10.1016/j.cej.2023.145909>.
- [139] D. Kokkinis, M. Schaffner, A.R. Studart, Multimaterial magnetically assisted 3D printing of composite materials, *Nat. Commun.* 6 (2015) 8643. <https://doi.org/10.1038/ncomms9643>.

- [140] Y.L. Kong, Multi-material 3D printing guided by machine vision, *Nature* 623 (2023) 488–490. <https://doi.org/10.1038/d41586-023-03420-9>.
- [141] W. Jung, Y.-H. Jung, P.V. Pikhitsa, J. Feng, Y. Yang, M. Kim, H.-Y. Tsai, T. Tanaka, J. Shin, K.-Y. Kim, H. Choi, J. Rho, M. Choi, Three-dimensional nanoprinting via charged aerosol jets, *Nature* 592 (2021) 54–59. <https://doi.org/10.1038/s41586-021-03353-1>.
- [142] J.T. Toombs, M. Luitz, C.C. Cook, S. Jenne, C.C. Li, B.E. Rapp, F. Kotz-Helmer, H.K. Taylor, Volumetric additive manufacturing of silica glass with microscale computed axial lithography, *Science* 376 (2022) 308–312. <https://doi.org/10.1126/science.abm6459>.
- [143] H. Wei, M. Lei, P. Zhang, J. Leng, Z. Zheng, Y. Yu, Orthogonal photochemistry-assisted printing of 3D tough and stretchable conductive hydrogels, *Nat. Commun.* 12 (2021) 2082. <https://doi.org/10.1038/s41467-021-21869-y>.
- [144] H. Wei, Q. Zhang, Y. Yao, L. Liu, Y. Liu, J. Leng, Direct-Write Fabrication of 4D Active Shape-Changing Structures Based on a Shape Memory Polymer and Its Nanocomposite, *ACS Appl. Mater. Interfaces* 9 (2017) 876–883. <https://doi.org/10.1021/acsami.6b12824>.
- [145] L. Liu, S. Liu, M. Schelp, X. Chen, Rapid 3D Printing of Bioinspired Hybrid Structures for High-Efficiency Fog Collection and Water Transportation, *ACS Appl. Mater. Interfaces* 13 (2021) 29122–29129. <https://doi.org/10.1021/acsami.1c05745>.
- [146] Z. Ji, C. Yan, S. Ma, S. Gorb, X. Jia, B. Yu, X. Wang, F. Zhou, 3D printing of bioinspired topographically oriented surfaces with frictional anisotropy for directional driving, *Tribol. Int.* 132 (2019) 99–107. <https://doi.org/10.1016/j.triboint.2018.12.010>.
- [147] Y. Liu, H. Zhang, P. Wang, Z. He, G. Dong, 3D-printed bionic superhydrophobic surface with petal-like microstructures for droplet manipulation, oil-water separation, and drag reduction, *Mater. Des.* 219 (2022) 110765. <https://doi.org/10.1016/j.matdes.2022.110765>.
- [148] P. Zhang, L. Zhang, H. Chen, Z. Dong, D. Zhang, Surfaces Inspired by the Nepenthes Peristome for Unidirectional Liquid Transport, *Adv. Mater.* 29 (2017) 1702995. <https://doi.org/10.1002/adma.201702995>.
- [149] L. Li, Y. Bai, L. Li, S. Wang, T. Zhang, A Superhydrophobic Smart Coating for Flexible and Wearable Sensing Electronics, *Adv Mater* 29 (2017) 1702517. <https://doi.org/10.1002/adma.201702517>.
- [150] L. Qin, Y. Wu, Z. Ma, H. Li, S. Lu, Z. Wang, J. Liu, M. Dong, Y. Zhang, Fluorine-Free and Highly Durable Superhydrophobic Textiles for Antifouling and Anti-icing Applications, *ACS Appl. Polym. Mater.* (2023) acsapm.3c00916. <https://doi.org/10.1021/acsapm.3c00916>.
- [151] M. Amin, M. Singh, K.R. Ravi, Fabrication of superhydrophobic PLA surfaces by tailoring FDM 3D printing and chemical etching process, *Appl. Surf. Sci.* 626 (2023) 157217. <https://doi.org/10.1016/j.apsusc.2023.157217>.

- [152] J. Long, M. Xi, P. Yang, Z. Huang, Mechanisms of metal wettability transition and fabrication of durable superwetting/superhydrophilic metal surfaces, *Appl. Surf. Sci.* 654 (2024) 159497. <https://doi.org/10.1016/j.apsusc.2024.159497>.
- [153] Z. Wu, C. Shi, Y. Li, A. Chen, L. Chen, B. Su, Abrasion-resistant superhydrophilic objects with anisotropic water transport capacities prepared by a selective laser sintering 3D printing strategy, *Chem. Eng. J.* 464 (2023) 142778. <https://doi.org/10.1016/j.cej.2023.142778>.
- [154] X. Zhang, Y. Yan, N. Li, P. Yang, Y. Yang, G. Duan, X. Wang, Y. Xu, Y. Li, A robust and 3D-printed solar evaporator based on naturally occurring molecules, *Sci. Bull.* 68 (2023) 203–213. <https://doi.org/10.1016/j.scib.2023.01.017>.
- [155] Z. Liu, Z. Zhan, T. Shen, N. Li, C. Zhang, C. Yu, C. Li, Y. Si, L. Jiang, Z. Dong, Dual-bionic superwetting gears with liquid directional steering for oil-water separation, *Nat. Commun.* 14 (2023) 4128. <https://doi.org/10.1038/s41467-023-39851-1>.
- [156] L. Xiao, G. Li, Y. Cai, Z. Cui, J. Fang, H. Cheng, Y. Zhang, T. Duan, H. Zang, H. Liu, S. Li, Z. Ni, Y. Hu, Programmable 3D printed wheat awn-like system for high-performance fogdrop collection, *Chem. Eng. J.* 399 (2020) 125139. <https://doi.org/10.1016/j.cej.2020.125139>.
- [157] Y. Shi, O. Ilic, H.A. Atwater, J.R. Greer, All-day fresh water harvesting by microstructured hydrogel membranes, *Nat. Commun.* 12 (2021) 2797. <https://doi.org/10.1038/s41467-021-23174-0>.
- [158] J. Yuan, X. Liu, O. Akbulut, J. Hu, S.L. Suib, J. Kong, F. Stellacci, Superwetting nanowire membranes for selective absorption, *Nat. Nanotechnol.* 3 (2008) 332–336. <https://doi.org/10.1038/nnano.2008.136>.
- [159] D. Yan, Y. Lu, J. Liu, Y. Chen, J. Sun, J. Song, Enhanced water transportation on a superhydrophilic serial cycloid-shaped pattern, *Nanoscale* 15 (2023) 11473–11481. <https://doi.org/10.1039/D3NR02180G>.
- [160] D. Wang, Q. Sun, M.J. Hokkanen, C. Zhang, F.-Y. Lin, Q. Liu, S.-P. Zhu, T. Zhou, Q. Chang, B. He, Q. Zhou, L. Chen, Z. Wang, R.H.A. Ras, X. Deng, Design of robust superhydrophobic surfaces, *Nature* 582 (2020) 55–59. <https://doi.org/10.1038/s41586-020-2331-8>.
- [161] Y. Xie, X. Qu, J. Li, D. Li, W. Wei, D. Hui, Q. Zhang, F. Meng, H. Yin, X. Xu, Y. Wang, L. Wang, Z. Zhou, Ultrafast physical bacterial inactivation and photocatalytic self-cleaning of ZnO nanoarrays for rapid and sustainable bactericidal applications, *Sci. Total Environ.* 738 (2020) 139714. <https://doi.org/10.1016/j.scitotenv.2020.139714>.
- [162] A. Elbourne, R.J. Crawford, E.P. Ivanova, Nano-structured antimicrobial surfaces: From nature to synthetic analogues, *J. Colloid Interface Sci.* 508 (2017) 603–616. <https://doi.org/10.1016/j.jcis.2017.07.021>.
- [163] L. Zhang, H. Chen, Y. Guo, Y. Wang, Y. Jiang, D. Zhang, L. Ma, J. Luo, L. Jiang, Micro–Nano Hierarchical Structure Enhanced Strong Wet Friction Surface Inspired by Tree Frogs, *Adv. Sci.* 7 (2020) 2001125. <https://doi.org/10.1002/advs.202001125>.

- [164] Y. Wang, X. Yang, Y. Chen, D.K. Wainwright, C.P. Kenaley, Z. Gong, Z. Liu, H. Liu, J. Guan, T. Wang, J.C. Weaver, R.J. Wood, L. Wen, A biorobotic adhesive disc for underwater hitchhiking inspired by the remora suckerfish, *Sci. Robot.* 2 (2017) eaan8072. <https://doi.org/10.1126/scirobotics.aan8072>.
- [165] T. Lan, H. Tian, X. Chen, X. Li, C. Wang, D. Wang, S. Li, G. Liu, X. Zhu, J. Shao, Treefrog-inspired Flexible Electrode with High Permeability, stable Adhesion, and Robust Durability, *Adv. Mater.* (2024) 2404761. <https://doi.org/10.1002/adma.202404761>.
- [166] M. Guo, Y. Wang, B. Gao, B. He, Shark Tooth-Inspired Microneedle Dressing for Intelligent Wound Management, *ACS Nano* 15 (2021) 15316–15327. <https://doi.org/10.1021/acsnano.1c06279>.
- [167] A.J. Shoffstall, S. Srinivasan, M. Willis, A.M. Stiller, M. Ecker, W.E. Voit, J.J. Pancrazio, J.R. Capadona, A Mosquito Inspired Strategy to Implant Microprobes into the Brain, *Sci. Rep.* 8 (2018) 122. <https://doi.org/10.1038/s41598-017-18522-4>.
- [168] Y. Yu, J. Guo, B. Ma, D. Zhang, Y. Zhao, Liquid metal-integrated ultra-elastic conductive microfibers from microfluidics for wearable electronics, *Sci. Bull.* 65 (2020) 1752–1759. <https://doi.org/10.1016/j.scib.2020.06.002>.
- [169] J. Ling, Z. Song, J. Wang, K. Chen, J. Li, S. Xu, L. Ren, Z. Chen, D. Jin, L. Jiang, Effect of honeybee stinger and its microstructured barbs on insertion and pull force, *J. Mech. Behav. Biomed. Mater.* 68 (2017) 173–179. <https://doi.org/10.1016/j.jmbbm.2017.01.040>.
- [170] N. Kröger, The Molecular Basis of Nacre Formation, *Science* 325 (2009) 1351–1352. <https://doi.org/10.1126/science.1177055>.
- [171] A.F. Demirörs, D. Courty, R. Libanori, A.R. Studart, Periodically microstructured composite films made by electric- and magnetic-directed colloidal assembly, *Proc. Natl. Acad. Sci.* 113 (2016) 4623–4628. <https://doi.org/10.1073/pnas.1524736113>.
- [172] C.D. Bandara, S. Singh, I.O. Afara, A. Wolff, T. Tesfamichael, K. Ostrikov, A. Oloyede, Bactericidal Effects of Natural Nanotopography of Dragonfly Wing on *Escherichia coli*, *ACS Appl. Mater. Interfaces* 9 (2017) 6746–6760. <https://doi.org/10.1021/acsami.6b13666>.
- [173] P. Kirya, E. Chen, M. Achterman, K. Eugenio, Z. Beshir, N. Ngoy, R.H. Siddique, A.O. Cakmak, J. Ashcroft, Biomimicry of Blue Morpho butterfly wings: An introduction to nanotechnology through an interdisciplinary science education module, *J. Soc. Inf. Disp.* 29 (2021) 896–915. <https://doi.org/10.1002/jsid.1071>.
- [174] E.M. Domingues, G. Gonçalves, B. Henriques, E. Pereira, P.A.A.P. Marques, High affinity of 3D spongin scaffold towards Hg(II) in real waters, *J. Hazard. Mater.* 407 (2021) 124807. <https://doi.org/10.1016/j.jhazmat.2020.124807>.
- [175] N.J. Mlot, C.A. Tovey, D.L. Hu, Fire ants self-assemble into waterproof rafts to survive floods, *Proc. Natl. Acad. Sci.* 108 (2011) 7669–7673. <https://doi.org/10.1073/pnas.1016658108>.

- [176] S. Stadlmayr, K. Peter, F. Millesi, A. Rad, S. Wolf, S. Mero, M. Zehl, A. Mentler, C. Gusenbauer, J. Konnerth, H.C. Schniepp, H. Lichtenegger, A. Naghilou, C. Radtke, Comparative Analysis of Various Spider Silks in Regard to Nerve Regeneration: Material Properties and Schwann Cell Response, *Adv. Healthc. Mater.* 13 (2024) 2302968. <https://doi.org/10.1002/adhm.202302968>.
- [177] H. Bagheri, A. Hu, S. Cummings, C. Roy, R. Casleton, A. Wan, N. Erjavić, S. Berman, M.M. Peet, D.M. Aukes, X. He, S.C. Pratt, R.E. Fisher, H. Marvi, New Insights on the Control and Function of Octopus Suckers, *Adv. Intell. Syst.* 2 (2020) 1900154. <https://doi.org/10.1002/aisy.201900154>.
- [178] Y. Wang, G. Sun, Y. He, K. Zhou, L. Zhu, Octopus-inspired sucker to absorb soft tissues: stiffness gradient and acetabular protuberance improve the adsorption effect, *Bioinspir. Biomim.* 17 (2022) 036005. <https://doi.org/10.1088/1748-3190/ac59c6>.